archive

PROCEEDINGS OF THE EIGHTH INTERNATIONAL
CLOSED-CYCLE SPECIALISTS' MEETING

Massachusetts Institute of Technology
Energy Laboratory
May 19-20, 1977

Sponsored by the US Department of Energy

Energy Laboratory Report No. MIT-EL 78-005
Approved for release March 1978

TABLE OF CONTENTS

TABLE OF CONTENTS (CONT'D.)

AGENDA

WORKSHOP OF

CLOSED CYCLE MHD SPECIALISTS

Massachusetts Institute of Technology
Cambridge, Massachusetts

Thursday, May 19, 1977

9:00   WELCOME AND OVERVIEW   J. F. Louis

        Remarks   V. Chernyshev

        Rand Status Report on Closed Cycle MHD   R. Y. Pei

        GENERATOR PERFORMANCE

        1. Recent Results of the Eindhoven Linear
            Generator   A. Veefkind

        2. Effect of Contaminants on Generator
            Performance   T. Dellinger

        3. MIT Disk Generator Results   W. Loubsky

        4. AVCO Disk Generator Results   J. Klepeis

        5. Review of Disk Performance   T. Nakamaura

2.00   PLASMA PHENOMENA

        1. Electrode Phenomena   H. Messerle

        2. Non-Uniformities and Reduction
            Formulae   S. Shamma

        3. Fluctuation Analysis   W. Hellebrekers

        4. GE Closed-Cycle Program   C. Marston

        5. Japanese Program   S. Shioda
                                                      M. Yoshimura

Friday, MAY 20, 1977

9:00   <u>FACILITIES AND SYSTEM STUDIES</u>

    1.   Dutch MHD Development Program   R. A. Van der Laken

    2.   Status of the Eindhoven Blow-Down
        Facility   J. H. Blom

    3.   Seeding of MHD Generators   I. Mostinsky

    4.   NASA Lewis Program in Closed-Cycle
        MHD   R. J. Sovie

    <u>ROUND-TABLE DISCUSSION</u>

FRIDAY AFTERNOON VISITS

    1.   MHD Combustion Facility   J. Cordero

    2.   MHD Disk Generator   W. Loubsky

    3.   Ceramic Electrode Fabrication
        Facility   R. Pober

ATTENDEES

George S. Argyropoulos
Massachusetts Institute of Technology
Energy Laboratory
Cambridge, Massachusetts 02139

V. T. Bitiurin
Institute of High Temperatures
Korovinskow Road
Moscow, USSR

J. H. Blom
Eindhoven University of Technology
Eindhoven, The Netherlands
Telephone: 040-474443

V. V. Chernyshev
I.A.E.A.
P.O. Box 590
Kartner Ring 11
Vienna, Austria
Telephone: 52-45-11 Ext. 7-31

T. C. Dellinger
General Electric Co.
Space Sciences Lab.
P.O. Box 8555
Philadelphia, PA 19101
Telephone: (215) 962-1389

Howard D. Cohen
Massachusetts Institute of Technology
Energy Laboratory
Cambridge, Massachusetts 02139
Telephone: (617) 253-3496

W. M. Hellebrekers
Eindhoven University of Technology
Eindhoven, The Netherlands
Telephone: 040-474498

James Klepeis
Avco
Everett, Massachusetts
Telephone: (617) 389-3000

William J. Loubsky
Massachusetts Institute of Technology
Energy Laboratory
Cambridge, Massachusetts 02139
Telephone: (617) 253-1759

Jean F. Louis
Massachusetts Institute of Technology
Energy Laboratory
Cambridge, Massachusetts 02139
Telephone: (617) 253-1760

Charles H. Marston
General Electric Co.
Room L9505, VFSC
P.O. BOX 8555
Philadelphia, Pa. 19101
Telephone: (215) 962-3493

H. K. Messerle
Electrical Engineering School
University of Sydney
Sydney 2006
NSW, Austrailia
Telephone: 6922565

I. Mostinsky
IVTAN
Moscow, USSR
Telephone: 273-28-86

Takashi Nakamura
Stanford University
HTGL Mechanical Engineering
Stanford University
Stanford, California 94305
Telephone: (415) 497-1745

Kazuo Onda
Electrotechnical Laboratory
5-4-1 Mukodai-Machi
Tanashi-Shi
Tokyo, Japan
Telephone: 0424-01-2141

R. Y. Pei
The Rand Corporation
2100 M Street NW
Washington, D.C. 20037
Telephone: (202) 296-5000

Alex Rodzianki
U.S.E.R.D.A.
FE/MHD
Washington, D.C. 20545

Marcos Rosenbaum
Massachusetts Institute of Technology
Energy Laboratory
Cambridge, Massachusetts 02139
Telephone: (617) 253-1781

Shawky Shamma
Massachusetts Institute of Technology
Aeronautics and Astronautics
Cambridge, Massachusetts 02139
Telephone: (617) 253-3764

Yu Sokolov
Institute for HIgh Temperatures
Academy of Sciences
Korovinskoe Road, 127412
Moscow, USSR
Telephone: 485-95-72

Ronald J. Sovie
NASA Lewis Research Center
2100 Brookpark Road
Cleveland, Ohio 44135
Telephone: (216) 433-4000 Ext. 6811

Tom Swean
STD Research Corporation
Washington, D.C.
Telephone: (202) 223-0422

J. Derek Teare
Massachusetts Institute of Technology
Energy Laboratory
Cambridge, Massachusetts 02139
Telephone: (617) 253-7067

Robert A. Van der Laken
Netherlands Energy Research Foundation (ECN)
Petten, Holland

Abraham Veefkind
Eindhoven University of Technology
Eindhoven, The Netherlands
Telephone: 40-474499

Jerome A. Vigil
Massachusetts Institute of Technology
Energy Laboratory
Cambridge, Massachusetts 02139
Telephone: (617) 253-1748

Masahiro Yoshimura
Massachusetts Institute of Technology
Material Science & Engineering
Cambridge, Massachusetts 02139
Telephone: (617) 253-6891

WELCOME AND OVERVIEW
by
Professor Jean F. Louis
Massachusetts Institute of Technology

Professor Louis welcomes the specialists from several countries around the world and from different American research centers to this workshop under the auspices of the MHD Liason Group and ERDA. Professor Louis remarks that these meetings were at least ten years old and had traditionally provided excellent opportunities for extensive exchanges of information. Professor Louis proposes an agenda which will cover the key items of interest in Closed MHD Power Generation. They are:

 a) generator performance

 b) properties and characteristics of non-equilibrium plasma

 c) description and performance of new facilities, system performance and review of future plans

 d) round-table discussion.

The detailed agenda, organized along these lines, was adapted.

Since the workshop is held under the auspices of the International Liason Group on MHD, he asks the representative of this group, Dr. Chernyshev, to address the meeting.

<u>REMARKS</u>

by

V. Chernyshev

I.A.E.A.

Vienna, Austria

Gentlemen,

It is a great pleasure for me to welcome all of you to the 1977 Closed-Cycle MHD Specialists Meeting.

As you know, this is the eighth in a series of annual meetings organized under the auspices of the Joint International Liaison Group on MHD Electrical Power Generator. This group is now sponsored by IAEA and UNESCO.

I hope that such an informal meeting just after the Sixteenth Symposium on Engineering Aspects in MHD will give a good opportunity for exchanging results and opinions on closed-cycle research, as compared with other achievements in the MHD field, and will involve more specialists in our discussion.

An important feature of such a meeting is a broad round-table discussion.

I would like to inform you on several international meetings which will deal with MHD in the coming year:

--World Electrotechnical Congress, June 21-25, 1977, Moscow, U.S.S.R.
--The Tenth World Energy Conference, September 19-24, 1977, Istanbul, Turkey
--International Advanced Course and Workshop on Thermodynamics of Magnetic Fluids, October 25-28, 1977, Udine, Italy
--Concerning the Seventh International Conference on MHD Electrical Power Generation, I would like to inform you that the recommendation of the Joint Liaison was to hold this meeting in 1977, most likely in Moscow, U.S.S.R.
--The next meeting of the Joint Liason Group planned for March 1977 should be held at IAEA Headquarters in Vienna

I would like again to express my hope that our meeting will be interesting and fruitful for all of us and will help to clarify benefits and future applications of Closed-Cycle MHD Systems.

Thank you.

RAND STATUS REPORT ON CLOSED-CYCLE MHD

by

R. Y. Pei

The Rand Corporation

Washington, D.C.

Comparison of Some ECAS Cost Estimates

The relative ranking of cost of electricity from ECAS MHD system studies was presented. The values are expressed as multiples of the advance steam plant COE.

The capital component is in then-year dollars and based on plants with different on-line dates. The capital charge rate of 18 percent reflects a 10 percent interest rate, which in turn reflects a 6.5 % inflation rate. This rate appears to be inconsistent with the assumption of constant fuel and O&M costs over a thirty-year life. To account for the increasing proportion of COE represented by fuel and O&M costs in an inflationary period, the 30-year inflation-levelized fuel and O&M costs have been derived.

The changes in the COE multiples for the fuel efficient systems improve significantly for the MHD systems. However, closed-cycle MHD is still thirty to seventy percent more costly than the advanced steam.

A status report was also given of the 1976-77 Rand assessment of closed-cycle MHD carried out for ERDA.

GENERATOR PERFORMANCE

EXPERIMENTS WITH THE EINDHOVEN MHD SHOCK-TUNNEL FACILITY

by

A. Veefkind

Eindhoven University of Technology

Eindhoven, Netherlands

The research with the shock-tunnel facility is directed towards two subjects: the experimental study of fluctuations and the behavior of the generator at inlet stagnation temperatures of 2000 K and lower. The former subject has been discussed before[1], the latter is considered in this presentation.

When the inlet stagnation temperature is decreased, a noticeable increase of the inlet relaxation length is observed (Figure 1).
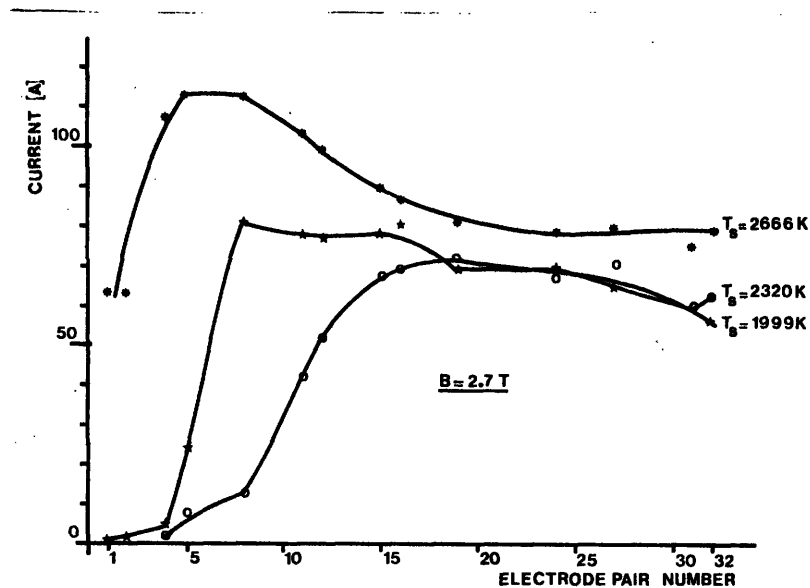

Figure 1. Load current vs. electrode pair number at different inlet stagnation temperatures.

The relaxation length could not be described, either by the quasi-one-dimensional analysis including finite ionization rates, or by two-dimensional analysis.

Increase of inlet relaxation length not only occurs as a result of decreasing inlet stagnation temperature; it also occurs when the magnetic induction is decreased[2] or when the impurity fraction is increased (Figures 2 and 3).

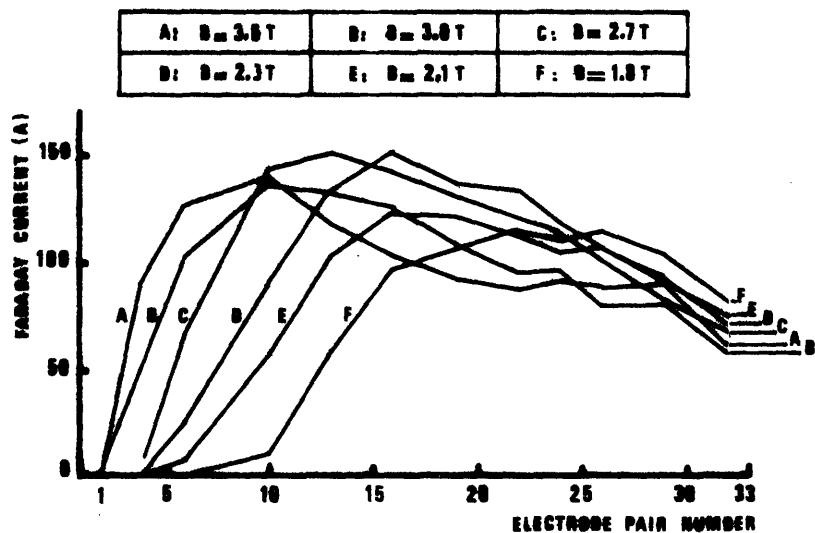| A: B=3.8 T | B: B=3.0 T | C: B=2.7 T |
| D: B=2.3 T | E: B=2.1 T | F: B=1.8 T |

Figure 2. Load current vs. electrode pair number at different magnetic inductions. T_S = 2200 K.
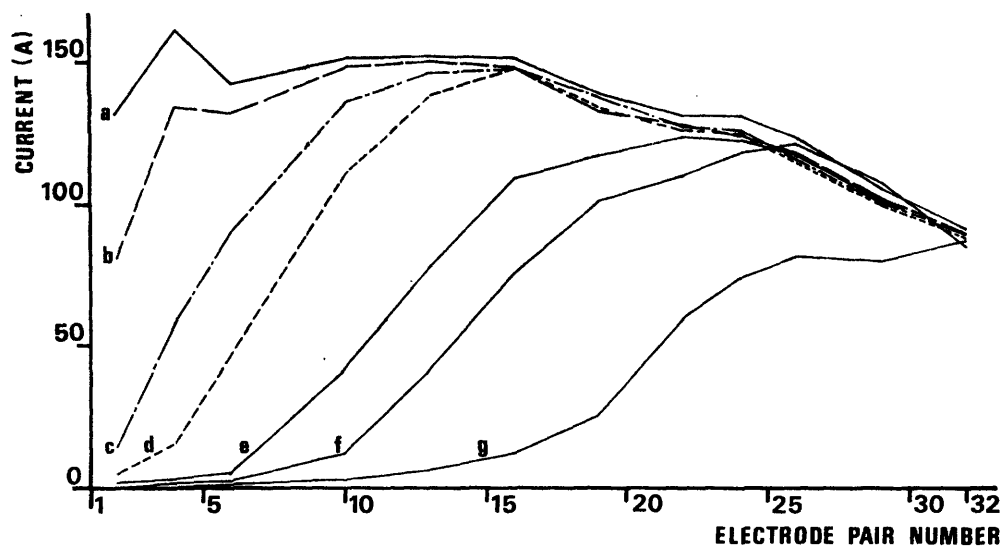

Figure 3. Load current vs. electrode pair number at different fractions of nitrogen impurity. T_S = 3500 K.

B = 2T

a.: 0%, b.: 0.09%, c.: 0.28%, d.: 0.45%, e.: 0.61%, f.: 0.8%, g.: 1.02%.

It is generally experienced that unexpected long relaxation lengths appear in situations where lower electron temperatures are expected.

The measurements at lower stagnation temperatures are also characterized by larger fluctuation levels, e.g., measured on the load current. It has been demonstrated by correlation techniques[1] that these fluctuations exist in the bulk of the plasma and that they are convected with the gasflow.

In spite of the appearance of longer relaxation lengths and larger fluctuation levels, an enthalpy extraction of 12% has been measured at an inlet stagnation temperature of 2000 K, at a magnetic induction of 3.3T. Future experiments will be performed to determine the lowest stagnation temperature at which a reasonable electrical conduction is possible. Other experiments will be directed to the influence of nitrogen and carbon dioxide contaminants on the generator performance at stagnation temperatures around 2000 K. About this subject, an exchange of experimental and theoretical data has been arranged with General Electric Company, King of Prussia, PA[3].

References

1. W. M. Hellebrekers, et al., "Experimental Fluctuation Analysis in a Noble Gas MHD Generator," Proc. 16th Symp. on Eng. Asp. of MHD, II.3.14, Pittsburgh, PA, 1977.

2. J. H. Blom, et al., "Enthalpy Extraction Experiments at Various Stagnation Tempertures in a Shock-Tunnel MHD Generator," Proc. 15th Symp. on Eng. Asp. of MHD, VI.5, Philadelphia, PA, 1976.

3. T. C. Dellinger, these proceedings.

EFFECT OF MOLECULAR CONTAMINANTS ON MHD GENERATOR PERFORMANCE

by

T. C. Dellinger
General Electric Company
King of Prussia, Pa.

A summary discussion is given here regarding a current analytical task to develop a model for predicting the effects of inelastic collisions involving molecular contaminants in the inert gas/alkali seed working fluid of a non-equilibrium, Closed Cycle MHD generator. The molecular contaminant species of prime interest are N_2, CO, CO_2, and H_2O, which are the major contaminant carryover species that have been measured in an experimental study of fossil fuel fired ceramic regenerative heat exchanger, which is used to heat an argon test gas[1]. Along with the contaminant species, the generator working fluid contains an inert gas such as argon, neutrals and ions of an alkali metal seed atom such as cesium or potassium and free electrons resulting from seed ionization. The presence of the molecular species provides an opportunity for inelastic energy transfer to occur with the particles resulting in excitation and deexcitation of the internal vibrational energy modes. The overall effect can be a reduction in the non-equilibrium electron temperature and a concurrent reduction in gas electrical conductivity, which affects generator performance.

To study these phenomena, a kinetic model approach is used in which an attempt has been made to identify the pertinent energy transfer mechanisms and to derive appropriate expressions for the energy transfer rates among all the various working fluid gas components. The energy transfer mechanisms considered include the following: (1) elastic energy transfer between electrons and heavy particles; (2) first level electronic excitation of seed atoms by electron impact; (3) vibrational excitation of molecular contaminant species by electron impact; (4) spontaneous emission of line radiation by the electronically excited seed

atoms; (5) quenching of the excited seed atoms by the vibration-
ally active molecular contaminants; (6) vibrational-translational
deexcitation of the vibrational energy of the molecular contami-
nants; (7) intra-molecular energy transfer between internal modes
of the triatomic contaminant species (CO_2 and H_2O); (8) inter-
molecular vibrational-vibrational energy transfer between dif-
ferent molecular contaminant species.

The expressions for the energy transfer rates depend upon
the model selected for the internal energy modes. For the vibra-
tional energy structure, the harmonic oscillator approximation is
used, and the nonequilibrium population densities are expressed
by a Boltzmann distribution in terms of a vibrational tempera-
ture. For the electronic internal energy of the seed atoms, only
the first excited level is considered, and its population is also
expressed using a Boltzmann distribution about a nonequilibrium,
excited state seed temperature. The model described above fol-
lows closely the approach of Bender, et al.[2], which is kinetic
analysis for a gas mixture of argon, seed (K, Na or Cs) and N_2
contaminant. The present work is an extension to CO, CO_2 and H_2O
contaminants and also involves some modifications to the energy
transfer rate formulations. The resonant quenching interaction
model of Ref. 2 has been replaced with a more general formulation,
taking into account the Ref. 3 quenching cross-section data given
as a function of the individual vibrational levels. Seed contri-
butions to the vibrational-translational relaxation time will
also be considered.

The planned work involves: (1) formulating the general kine-
tic model; (2) obtaining solutions for the steady-state approxi-
mation (algebraic equations); (3) incorporating the steady-state
analysis in an existing 1-D MHD generator code; and (4) deter-
mining the relaxation phenomena by solving the differential equa-
tions of the general kinetic model. The current status is that
items (1) and (2) are essentially complete except for continuing
work on the kinetic model for H_2O. Steady-state checkout calcu-
lations have been made for comparison with experimental data and
the theoretical predictions of other workers for conductivities

and temperatures for cases with and without N_2 and excellent agreement of the present analysis results with these data have been obtained. This provides confidence for considering cases with contaminants other than N_2, and for proceeding to the planned work items (3) and (4). As part of the planned work, calculations will be made to compare the experimental shock-tunnel contaminant effects data of the Netherlands Eindhoven University Closed Cycle MHD group. Preliminary data for the effects of N_2 and CO_2 were received from A. Veefkind at this Closed Cycle Specialists Meeting. At the same time, the author made available to the Netherlands group detailed descriptions of the theoretical modeling effort for contaminant effects. This interchange of information and cooperation is considered very helpful and is warmly welcomed. A continued fruitful, cooperative working arrangement is anticipated between the General Electric and Netherlands Closed-Cycle MHD efforts.

References

1. Cook, C.S., and Dickinson, K.M., "Argon Contamination Associated with Ceramic Regenerative Heat Exchangers for Closed Cycle MHD", 16th Symposium, Engineering Aspects of MHD, Univ. of Pittsburgh, Pittsburgh, Pa., May 1977.

2. Bender, D.J., et al., "Thermodyamic Nonequilibrium in an Argon, Nitrogen, Alkali-Seed Plasma," 5th International Conference on MHD Electrical Power Generation, Munich, Germany, 1971.

3. Fisher, E.R. and Smith, G.K., "Vibration-Electronic Coupling in the Quenching of Electronically Excited Alkali Atoms by Diatomics", Applied Optics, Vol. 10, No. 8, August 1971, pp. 1803-1813.

MIT DISK GENERATOR WITH SWIRL

by

W. J. Loubsky, J. K. Lytle, and J. F. Louis

Massachusetts Institute of Technology

Cambridge, Massachusetts 02139

A. Introduction

The advantages of the disk geometry over more conventional linear generators are numerous. Serious plasma and material limitations associated with the multiple electrodes of linear devices are eliminated. Since the disk is made of only two insulating walls, higher electric fields can be sustained and greater power densities can be achieved relative to the linear counterpart[1]. Moreover, the symmetry of the disk geometry affords simplicity of channel and superconducting magnet design.

When operating in the radial flow mode, the disk is a pure Hall-effect device. However, it has been demonstrated theoretically that a combination of radial flow with inlet swirl opposing the azimuthal Lorentz force can substantially increase the disk's turbine and electrical efficiency[1,2]. At Hall coefficients lower than five, the disk generator with swirl is expected to have better performance than the radial (Hall) configuration. The configuration is the circular (electrodeless) equivalent of a diagonally-connected Faraday generator.

The performance and efficiency of a small disk generator with 45° inlet swirl are presented. Electrical and thermodynamic properties measured in the generator plasma are analyzed.

B. MIT Swirl Generator

A scale drawing of the generator channel is shown in Figure 1. An entrance swirl of 45° is provided by twenty-four aerodynamically-designed swirl vanes which simultaneously expand the flow to a Mach number of 2.2. The vanes are electrically conducting, although isolated from all other components of the generator. The generator walls are instrumented with sixteen electric field probes and ports for static and stagnation pressure and electron

density measurements. The channel height is 1.25 in. with an inner radius of 3.5 in. and a generator volume of 118 in^3 (2 liters). Details of the generator design and facility system in general are described in Reference 3.

C. Experiments

Performance tests were made in argon ($\delta\tau_{eff} < 2.0$) for stagnation conditions 1950K $\leq T_o \leq$ 3350K and 6.7 atm $\leq p_o \leq$ 8.9 atm. The load resistance ranged from 0.029Ω $\leq R_L \leq \infty$ for B = 3.0 Tesla. Mass flow rates between 3.5 kg/sec $\leq$ m $\leq$ 4.7 kg/sec were provided, for a nominal test time of 3 msec, by a 15 cm reflected shock tunnel. Cesium was used as seed (nominally 0.35% Cs in Argon for all tests). Measurements were made of the (a) voltage and static pressure distributions in the generator, (b) stagnation pressure and electron density at the generator exit, and (c) swirl vane and electrode voltages. The generator flow luminosity was recorded with a high-speed framing camera (3000 frames/sec).

Figure 2 partially illustrates the data recorded during a typical run (R_L = 0.54Ω, Run #109). The test time relative to the magnetic field pulse is shown in Figure 2a, the indicator being the output of a Kistler PZT transducer (lower beam) located in the upstream portion of the shock tube. Up to nine electric field probes are used during any one run. Five were used for this example. The output voltage, defined as the difference between anode to ground and cathode to ground, and probe voltages are shown in Figures 2b and 2c. In addition to the voltage trace in Figure 2c, two of the four static pressure histories and the swirl vane potential history are shown. The shape of the voltage and pressure histories suggests that the flow in the generator is steady during the entire test time.

The radial voltage and static pressure distributions (along a streamline; ports #1, 2, 3, 4 of Figure 1) for Run #109 are shown in Figure 3. The blade potential (-230 volts) is indicated in the figure. These data reveal several important facts about the generator flow. First, the ionization length is short when compared to generator length. Therefore, the performance is not
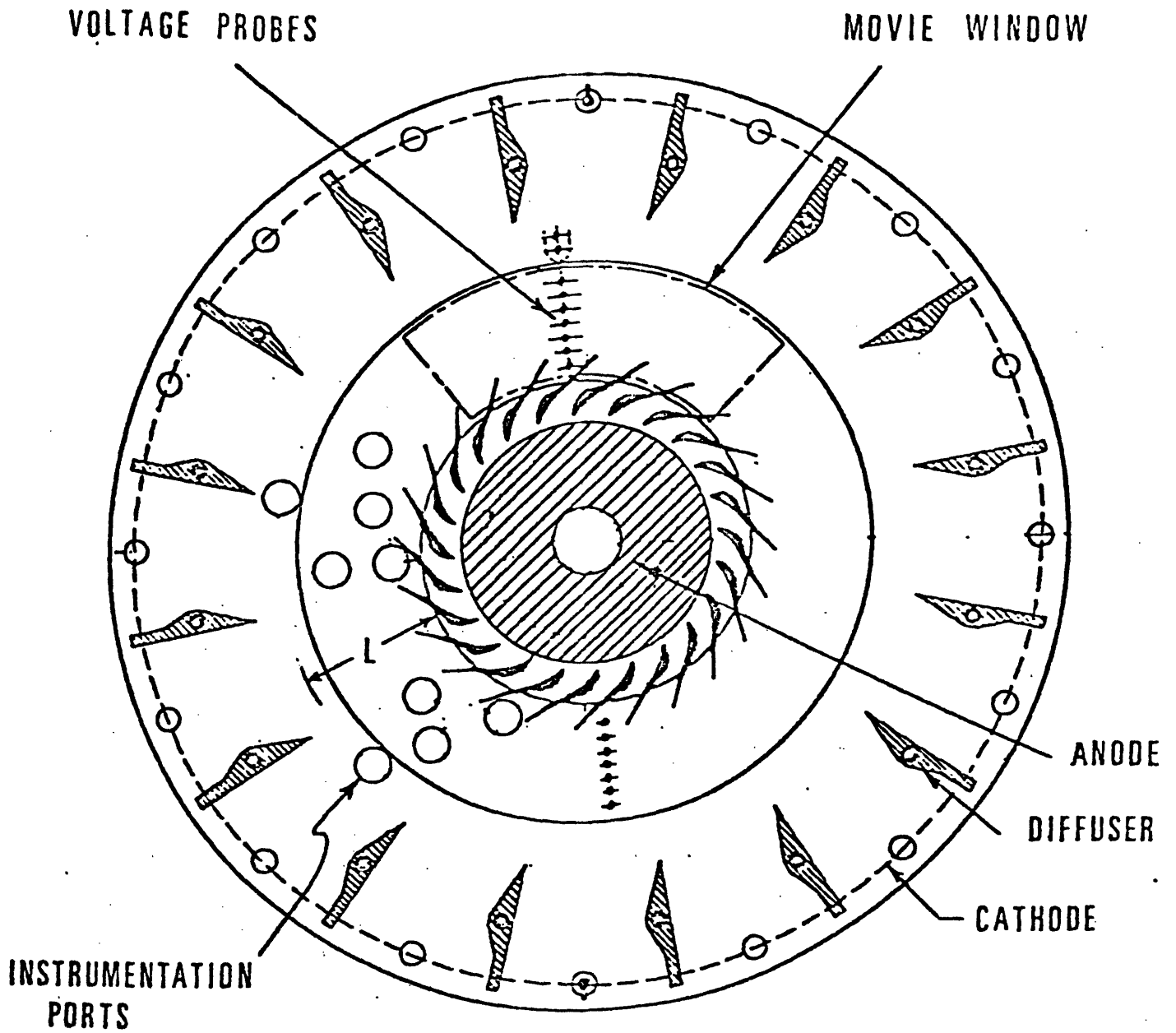
Figure 1   Layout of the Swirl Generator - View from the Inside of
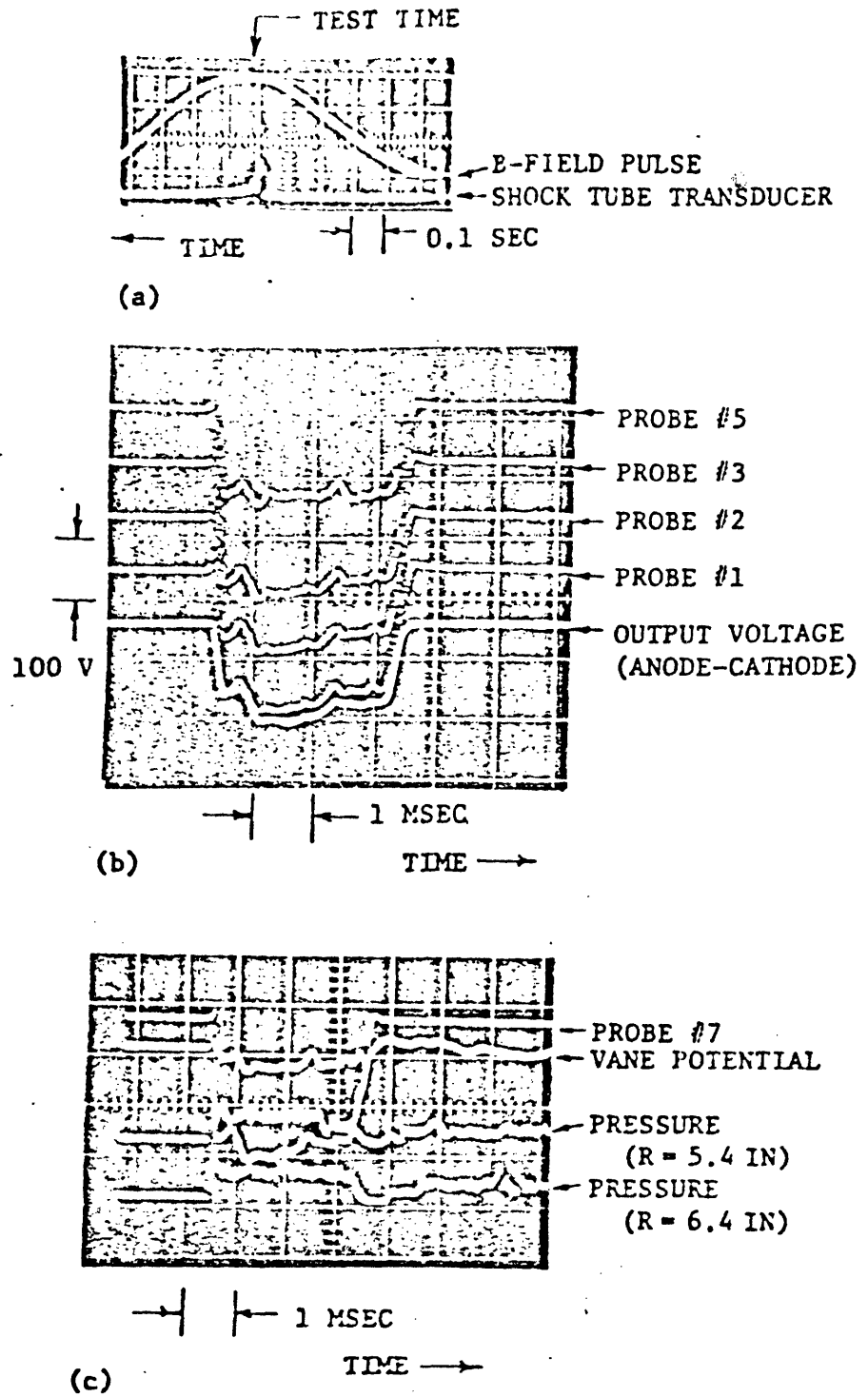the Generator on the Downstream Wall

FIGURE 2. DATA HISTORIES FOR A TYPICAL RUN
B_{max} = 3.0 Tesla, R_L = .054Ω, T_o = 2550°K, P_o = 8.6 atm.

appreciably affected by ionization relaxation. The swirl vanes float at the highest potential in the generator plasma. The vane trailing edge makes good electrical contact with the plasma via the trailing edge base flow. This suggests that no current flows through the vanes (an important design consideration for a steady-state generator). The plasma luminosity photographs bear out this fact. Figure 4 is a print of one frame ($\Delta\tau$ = 330 msec) of the movie taken during Run #109. The camera viewing window (see Figure 1) was chosen to include the flow between six swirl vanes (blades). The plasma is luminous between the vanes (where $j_\theta = 0$). This luminosity appears to emanate from the suction side of each blade where expansion is rapid and electronic heating occurs first. The pressure side of the blades remains dark where the plasma pressure remains high and electronic heating is small. For the case of open circuit ($j_r = 0$), no radiation is observed between the vanes for the same camera f_{stop} = 22.0. In general, the flow visualization results clearly reveal (a) the existence of wakes and trailing edge shocks behind each swirl vane blade and (b) the existence of an oblique shock in the generator as a result of the flow retarding force $j_\theta B$ (acting radially inward). The shock has good circular symmetry, and its position in the generator correlates well with the static pressure measurements. This last point can be seen, for example, by comparing the shock location (radiation ring) of Figure 4 with the pressure distribution shown in Figure 3. Since the shock is oblique to the flow, an increase in swirl angle is expected and is suggested by the wake deflection observed in Figure 4. No circular shock is observed when the magnetic field is not applied. For the photograph in Figure 5, the lens aperture was wide open (f_{stop} = 2.7). Since there is no current flow, the only plasma luminosity is that produced by the slowly expanding plasma on the pressure side of the blades, as compared to the suction side where the fast expansion results in a faster cooling of the plasma.
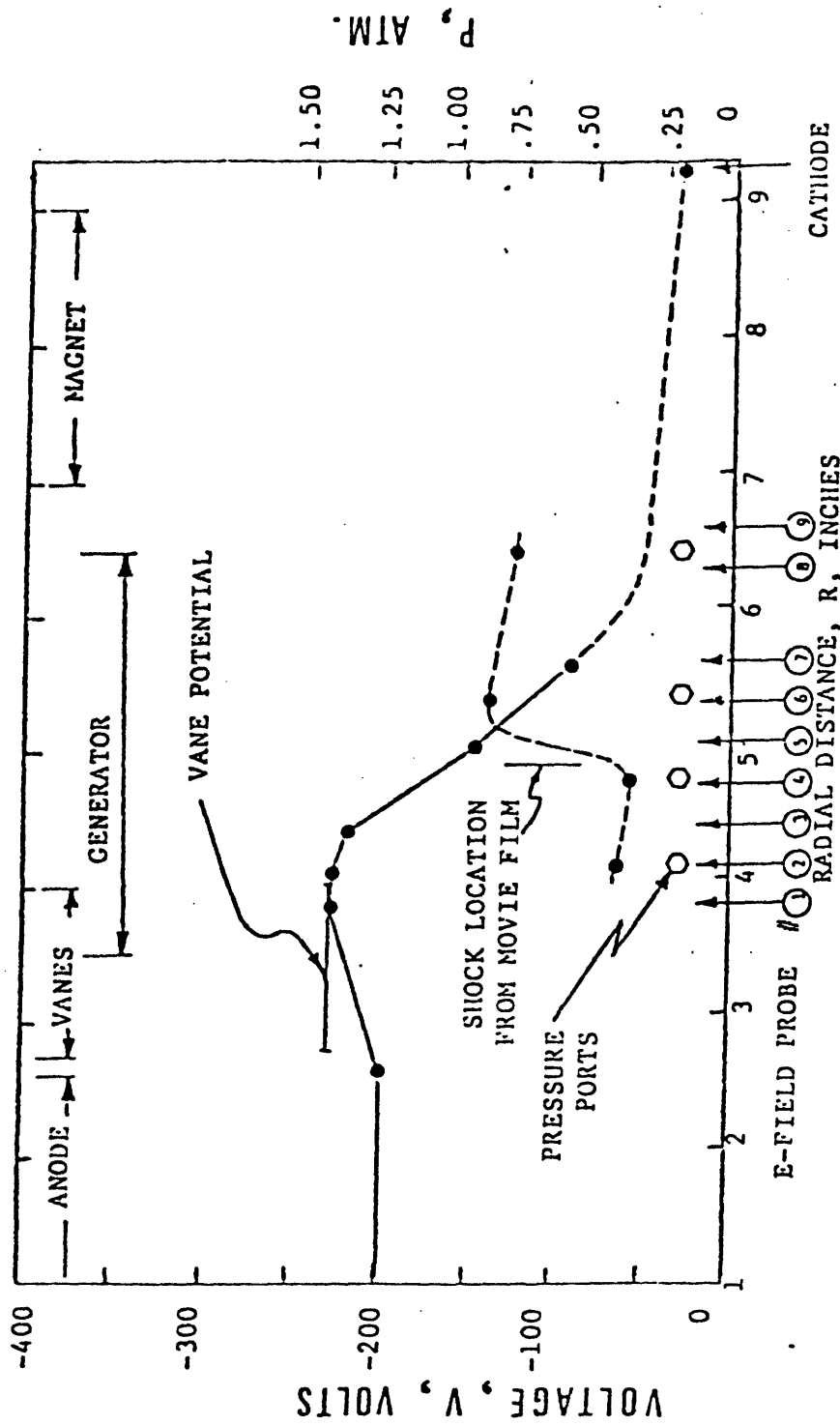
FIGURE 3. RADIAL VOLTAGE AND PRESSURE PROFILES: $T_0 = 2600°K$, $P_0 = 8.6$ atm., $\dot{m} = 4.6$ kg/sec., $B = 3.0$ T, $R_L = 054 \, \Omega$
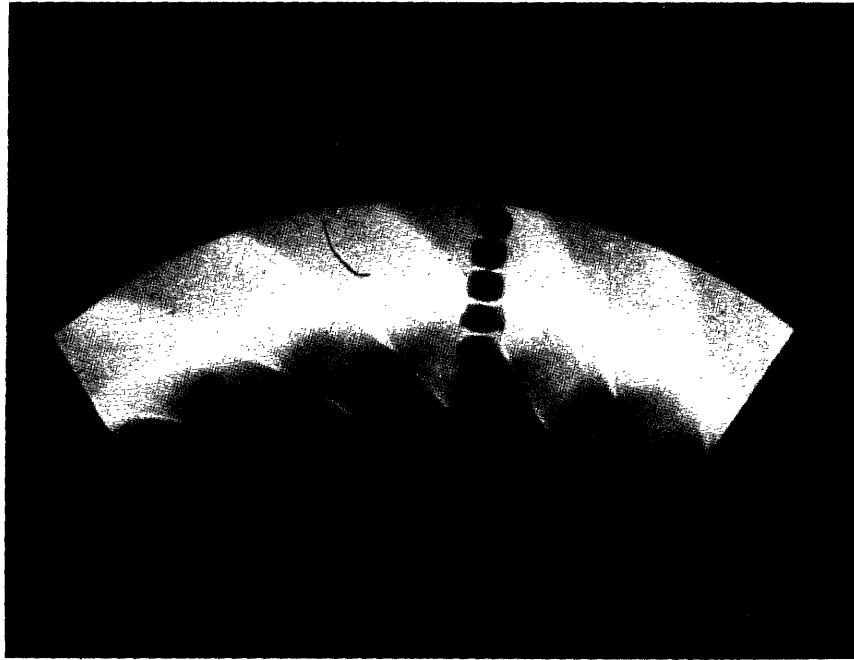
FIGURE 4. Photograph of the Plasma Luminosity in the
           Generator during the Interaction Test Time,
           Exposure 330 μsec.
           Test conditions: T_o = 255o°K, p_o = 8.6 atm,
           $\dot{m}$ = 4.6 kg/sec, P = 500 KW, $\eta_{er.}$ = 9.3%.
           Run #109

FIGURE 5. Photograph of the Plasma Luminosity in
          the Generator for the case of B = 0.

          Exposure 330 μsec.

          Test conditions: T_o = 2650 $^{\circ}$K, p_o = 8.6 atm,

          f_{stop} = 2.7

           Run # 118

The effect of stagnation temperature, T_o, on the voltage and pressure distributions in the generator is shown in Figure 6. Three things are noted. First, the inlet dissipation resulting in the plasma ionization is greater for the lower T_o case and the ionization relaxation time is slightly longer. After ionization relaxation, the E-field strength for both cases is comparable. The interaction is stronger for the higher T_o run as evidenced by the position of the circular shock in the generator, for a given load.

The effect of load resistance, R_L, on the voltage distribution in the generator is shown in Figure 7. The generator stagnation conditions were nominally T_o = 3075K and p_o = 8.25 atm. Qualitatively, the voltage profiles are similar to the ones obtained with the radial flow generator[3,4], i.e., a reversal of E-field is observed as R_L decreases. The static pressure distributions are shown in Figure 8. These data illustrate that the shocks present in the generator are relatively weak and the shock strength decreases with load resistance. The shocks do not appreciably affect the voltage distribution in the generator.

D. Performance

1. Power Output

The power output as a function of load resistance is shown in Figure 9 for two values of stagnation temperature. The peak power at T_o = 3075K is difficult to define (dotted line), since the peak is very sharp and the generator impedance varies slightly from run to run. However, the maximum power generated was over 900 kW (470 MW/m^3) with an enthalpy extraction of 17.2% (R_L = 0.029Ω). At T_o = 2000K, a peak power of 210 kW (105 MW/m^3) is obtained near R_L = 0.05Ω. The maximum enthalpy extracted at this temperature is 5.5%.

The effect of stagnation temperature on the power generated and the enthalpy extracted is shown in Figures 10 and 11 for a load resistance of R_L = .054Ω. At 1950K the power density is 100 MW/m^3, and at 3350K the output increased to 450 MW/m^3. These results, when compared with the Eindhoven experiments, illustrate
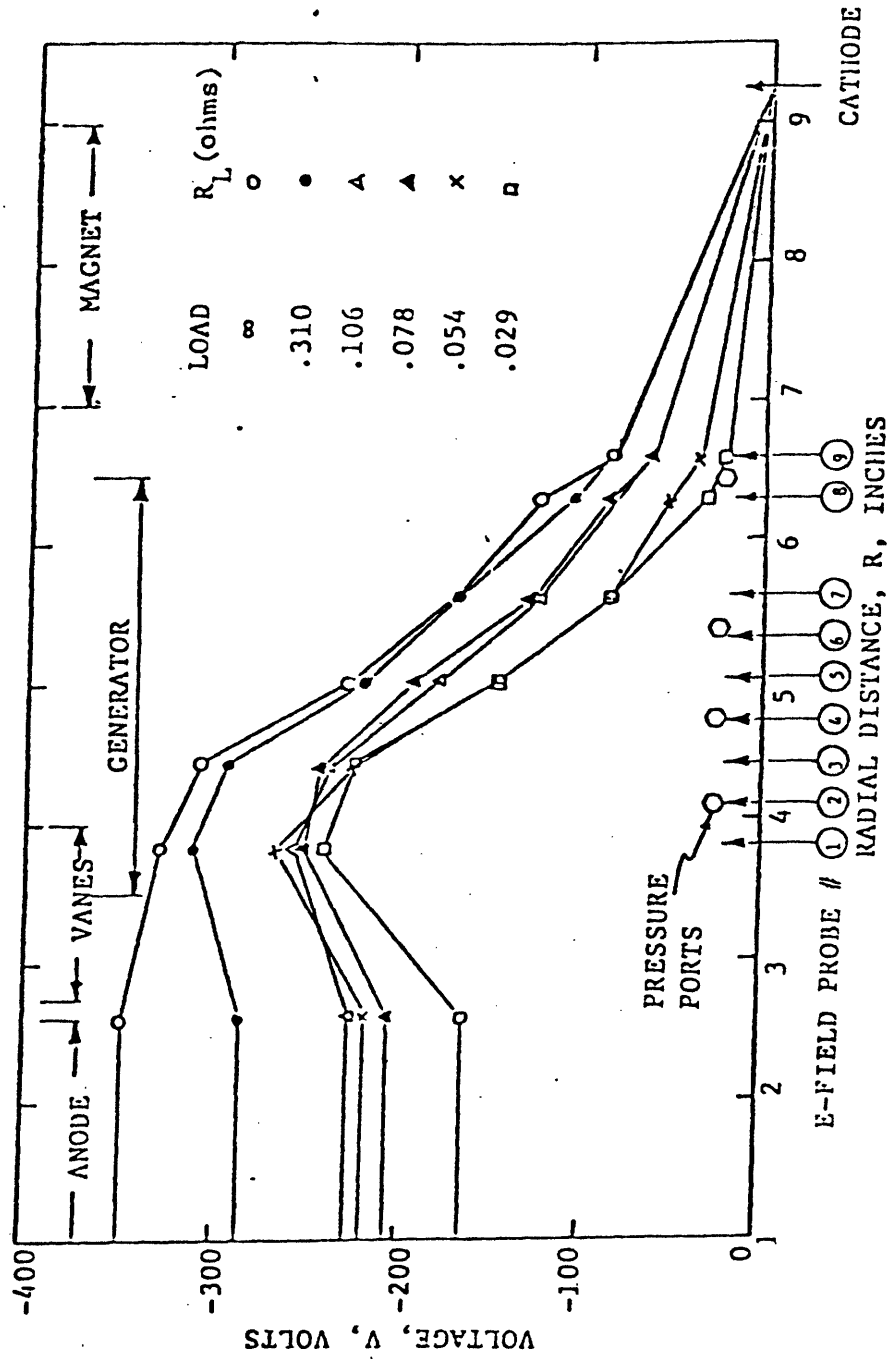
FIGURE 7   EFFECT OF LOAD ON GENERATOR VOLTAGE DISTRIBUTION
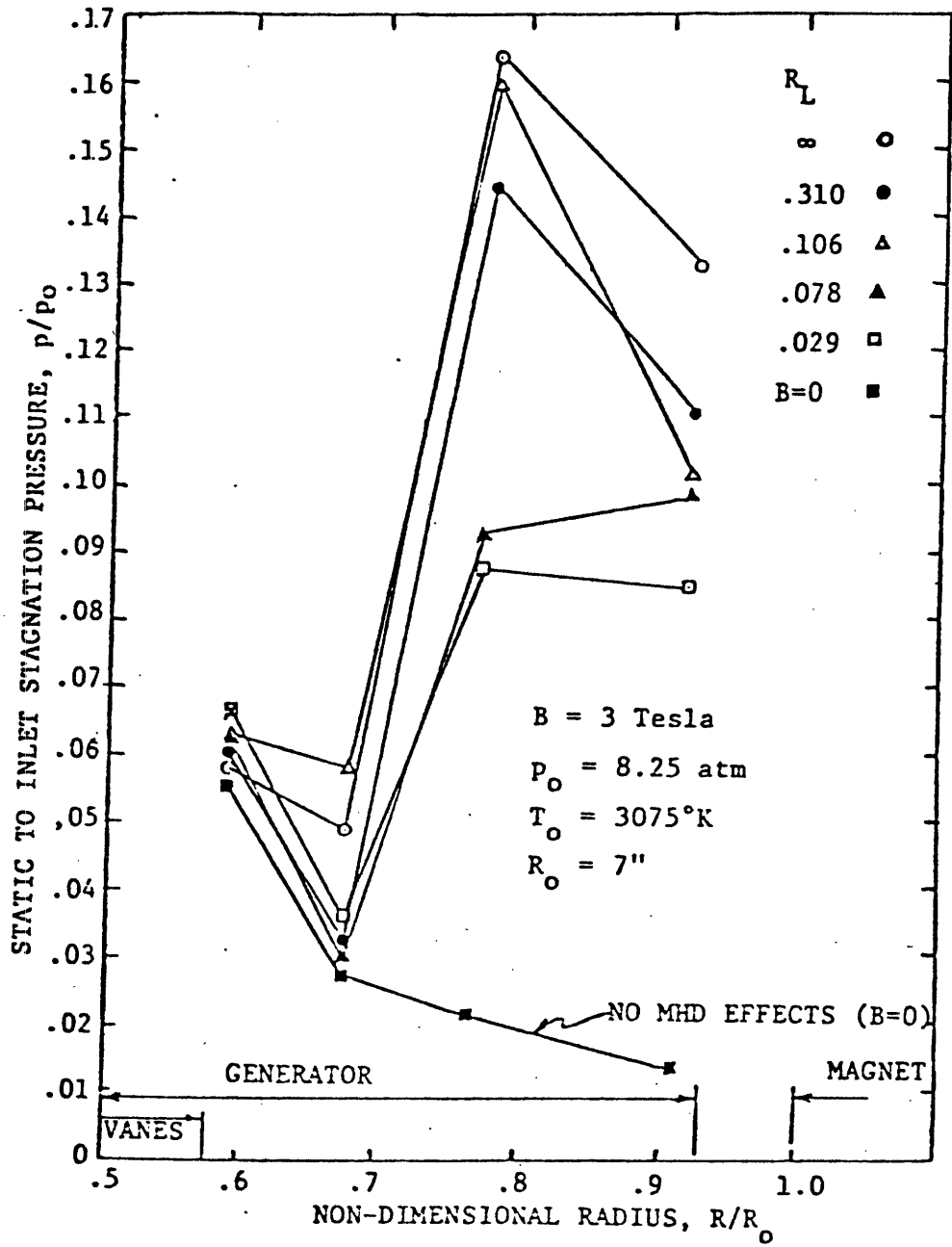$B = 3.0$ Tesla. Stagnation conditions: $P_o = 8.25$ atm., $T_o \approx 3075°K$

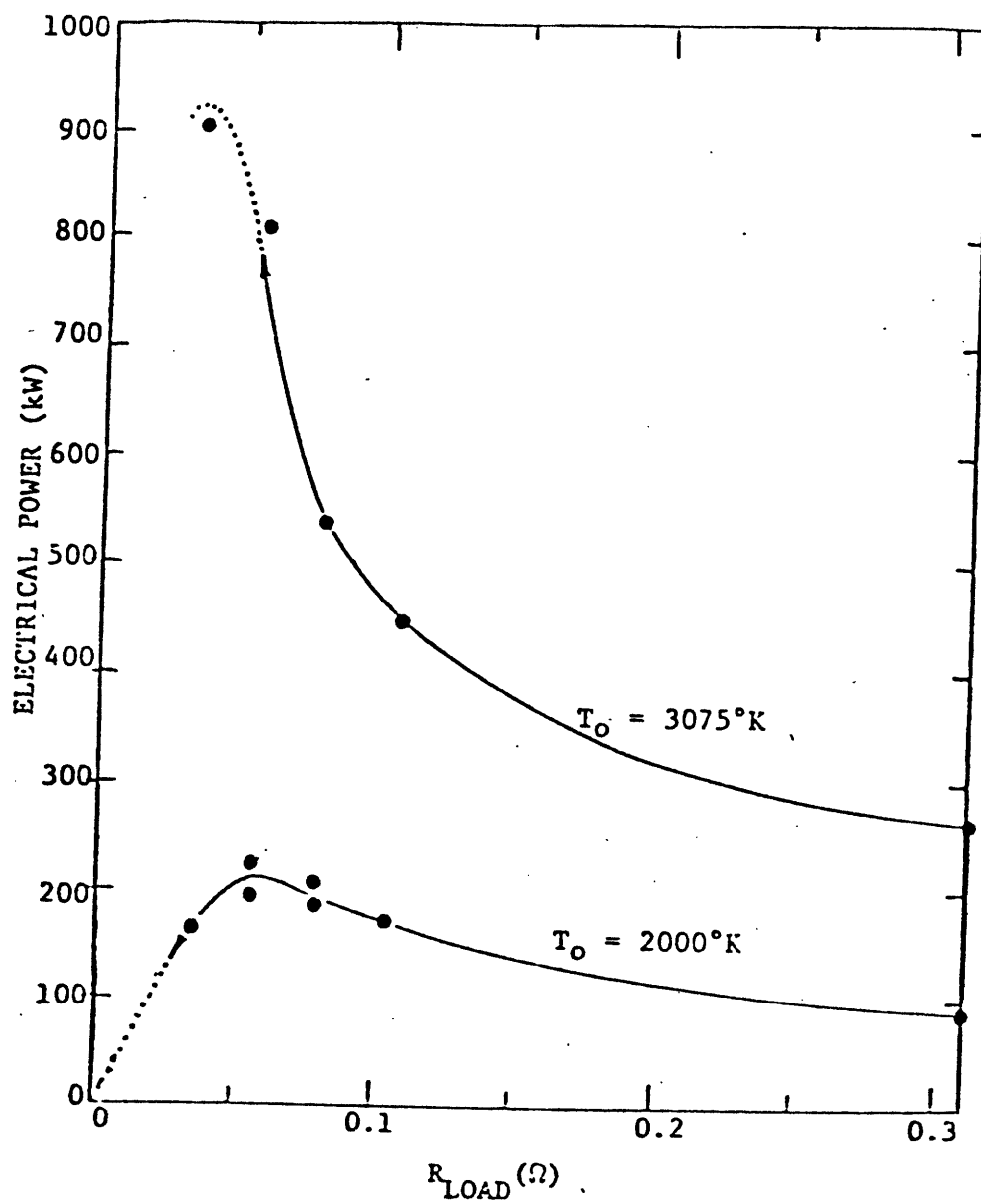FIGURE 8   EFFECT OF LOAD ON STATIC PRESSURE DISTRIBUTION

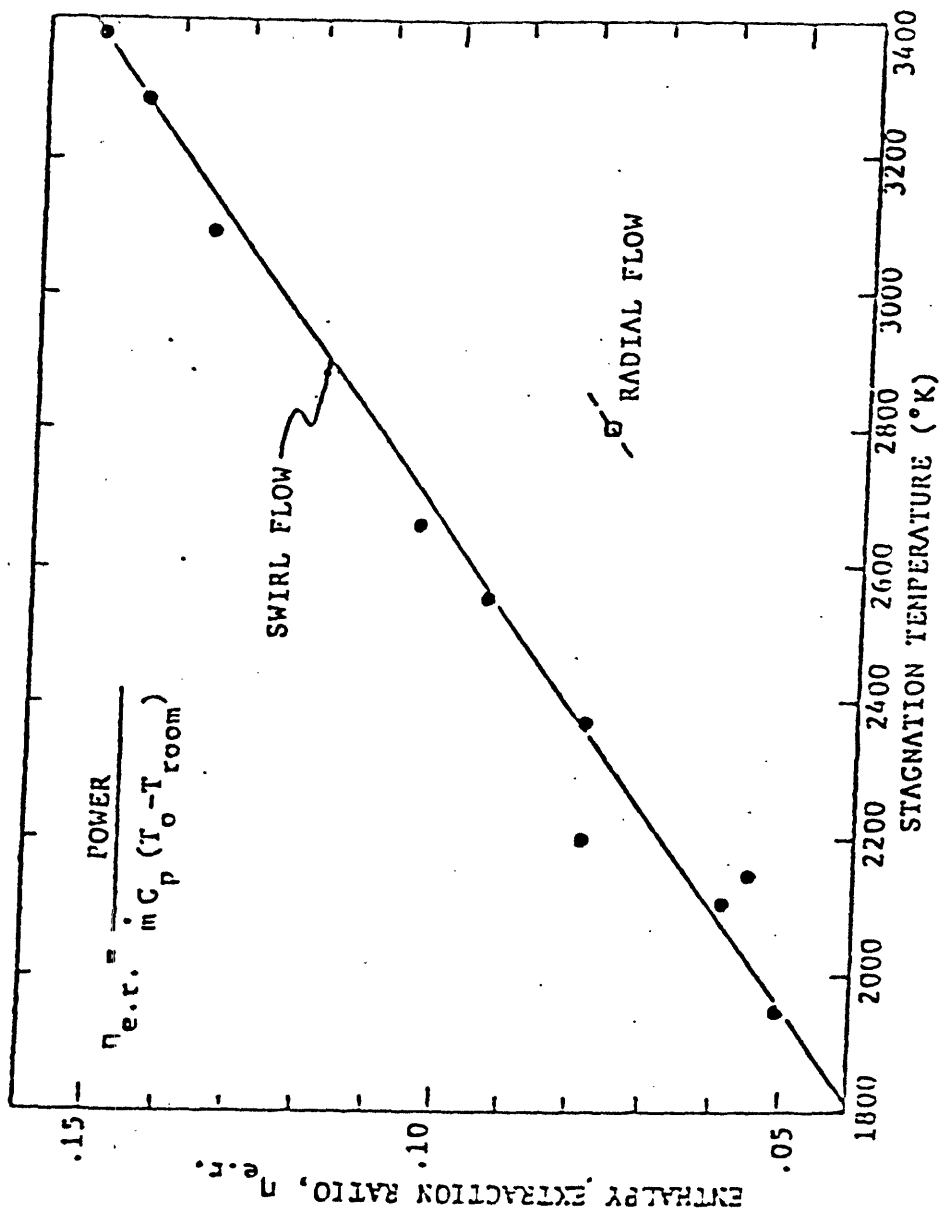FIGURE 9   ELECTRIC POWER VERSUS LOAD.

B = 3.0 Tesla, p_o = 8.2 atm.

FIGURE 11 ENTHALPY EXTRACTION RATIO VERSUS STAGNATION TEMPERATURE

$B = 3.0$ Tesla, $R_L = .054\Omega$

the enhanced performance of the disk over the linear Faraday generator[5]. For nearly the same stagnation conditions (T_o = 3300K, p_o = 7.2 atm) and mass flow rate (m = 3.4 kg/sec) the linear generator provided only about 95 MW/m^3 with an enthalpy extraction between 14-18% at B = 3.0 Tesla (5). The radial (Hall) flow result shown in Figures 10 and 11 also illustrates the advantage of inlet swirl on the performance of the disk. The generator voltage distribution in Figure 12 shows that 45° inlet swirl increases the E-field strength by 65% at T_o = 2730K.

2. Efficiency and Effective Hall Parameter

In order to completely evaluate the generator performance, the efficiency and effective Hall parameter must be determined. Theory predicts a substantial improvement in electrical effi- ciency with swirl, e.g., over a factor of two increase over the radial flow generator for 45° swirl with $\omega\tau_{eff}$ < 2.00 (see Figure 16). To determine the efficiency, the stagnation pressure in the generator must be measured. An average turbine (isentropic) efficiency is defined as

$$\eta_T = \frac{\Delta H_o(\text{actual})}{\Delta H_o(\text{isentropic})}$$

where ΔH_o (actual) is the difference between initial (entrance) and final (exit) total enthalpies in the generator for the actual process which includes losses due to friction, heat transfer to the walls, and Joule dissipation. ΔH_o (isentropic) is this dif- ference if the energy extraction process were reversible and adiabatic. The turbine efficiency can be expressed in terms of the enthalpy extraction ratio, $\eta_{e.r.}$, and the stagnation pressure ratio, i.e.,

$$\eta_T = \frac{\eta_{e.r.}(1 - \frac{T_{room}}{T_o})}{1 - (\frac{p'_o}{p_o})^{\frac{\gamma-1}{\gamma}}},$$

where p_o and T_o are the initial stagnation conditions and p'_o is the final stagnation pressure at the generator exit. γ is the ratio of specific heats, which for argon is = 1.66.
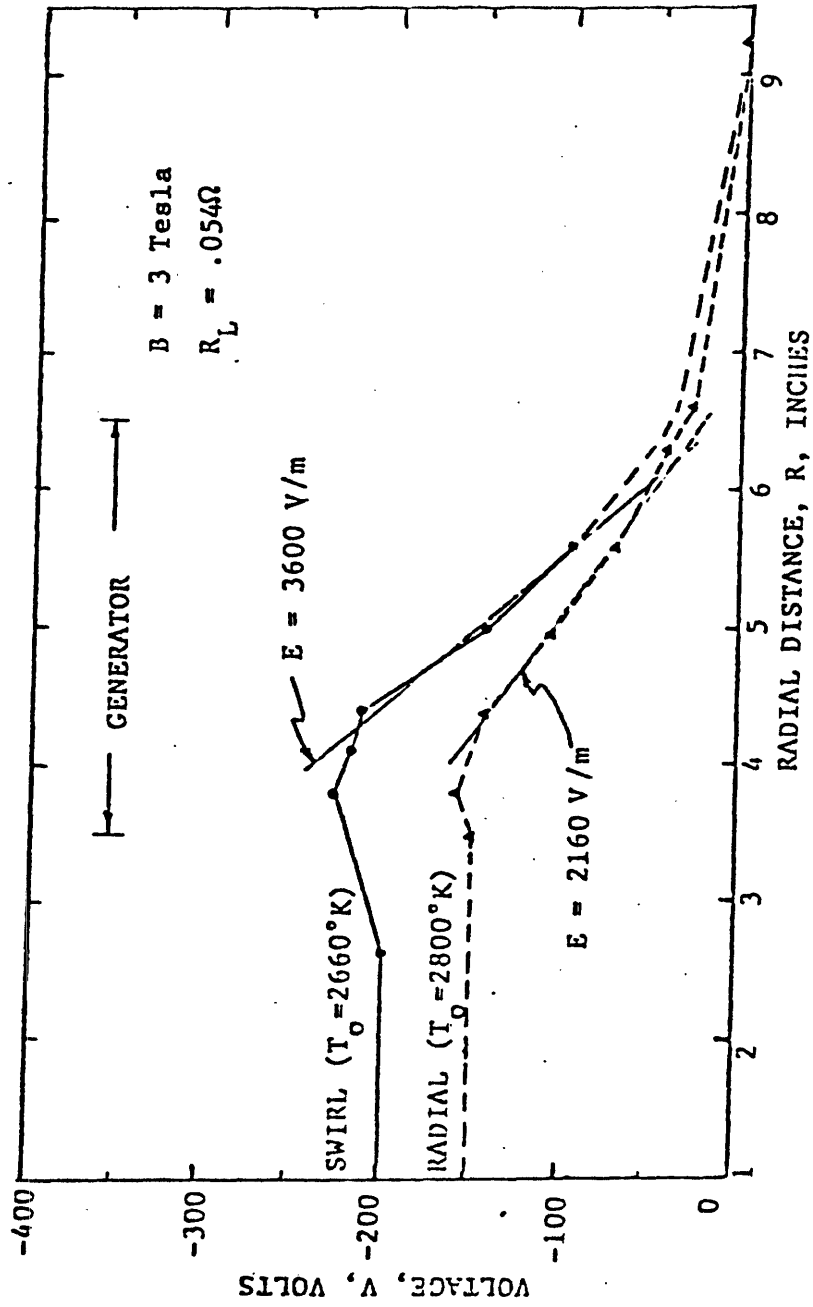
FIGURE 12   COMPARISON OF SWIRL AND RADIAL GENERATOR VOLTAGE DISTRIBUTIONS

The stagnation pressure is measured with a modified PZT transducer. The construction consists of a thin-walled pitot tube adapted to a standard Kistler gauge, the crystal located in the side wall of the generator. Prior to installation in the generator, the probe was calibrated in the shock tube under conditions of similar Mach number and pressure. The dynamic response of this probe was found to be small relative to the steady-flow test time. Angle of attack effects on the signal output are negligible up to $\alpha = 22^{\circ}$. The signal decreases for $\alpha > 22^{\circ}$, up to 15% at $\alpha = 45^{\circ}$. Consequently, angle of attack effects for measurements in the generator are negligible since the probe's angular position can be determined from the flow visualization (movie) results.

Two series of tests were conducted to evaluate the efficiency of the generator as a function of load. The initial stagnation conditions were $T_o = 3350K$, $p_o = 8.0$ atm and $T_o = 2450K$, $p_o = 6.7$ atm. The stagnation pressure probe was located midstream at the generator exit (port #4, see Figure 1), its axis orientated in the flow direction (45° from the radius). The exit static pressure was measured as well, since both p'_o and p are necessary in order to determine the local Mach number and the Rayleigh-Pitot correction factor (less than 10% for these conditions). Since the flow Mach number distribution in the generator is not determined, the local value (which approximates an average value) was used in the relationship between electrical efficiency, η_E, and η_T, i.e.,

$$\eta_E \equiv \frac{\eta_T(1 + \frac{\gamma-1}{2} M^2)}{1 + \frac{\gamma-1}{2} M^2 \eta_T} \qquad \text{(Reference 6)}$$

The electrical and turbine efficiencies versus load for these tests are shown in Figures 13 and 14. The enthalpy extraction ratio is also included in the figures. At $T_o = 3350K$, a

maximum turbine efficiency of η_T = 51% and a maximum electrical efficiency of η_E = 62% were obtained for R_L = .039Ω. Since the generator impedance varies slightly from run to run and the peak in the efficiency curve is very sharp, some scatter in the data is found near peak load. At T_O = 2450K, the maximum efficiencies found were η_E = 32%, η_T = 21% for a load resistance R_L = .053Ω.

In order to compare the efficiency data with the local theoretical predictions, the effective Hall parameter, $\omega\tau_{eff}$, for these tests must be determined. The method of accomplishing this is summarized as follows. For open-circuit conditions, the radial component of Ohm's Law yields

$$E_R = u_R B (K + \omega\tau_{eff}),$$

where E_R, u_R, and K are the local values of the radial electrical field, radial velocity, and swirl ratio, respectively. Solving for $\omega\tau_{eff}$ with K = 1.0 (45° swirl) this becomes

$$\omega\tau_{eff} = \frac{\sqrt{2}\ E_R}{uB} - 1 \qquad (1)$$

where the total velocity, u = $\sqrt{2}\ u_R$. To determine the flow velocity, three additional equations are needed. They are

$$\frac{P_o}{p} = (1 + \frac{\gamma-1}{2} M^2)^{\frac{\gamma}{\gamma-1}} \qquad (2)$$

$$\frac{P_o}{p} = (\frac{T_o}{T})^{\frac{\gamma}{\gamma-1}} \qquad (3)$$

$$\eta_T \equiv \frac{\Delta H_o (\text{ACTUAL})}{\Delta H_o (\text{ISENTROPIC})}$$

$$\eta_E \equiv \frac{\text{POWER}}{\text{POWER} + j^2/\sigma}$$

η_E (ELECTRICAL)

η_T (TURBINE)

$\eta_{e.r.}$ (ENT.EXT.RATIO)
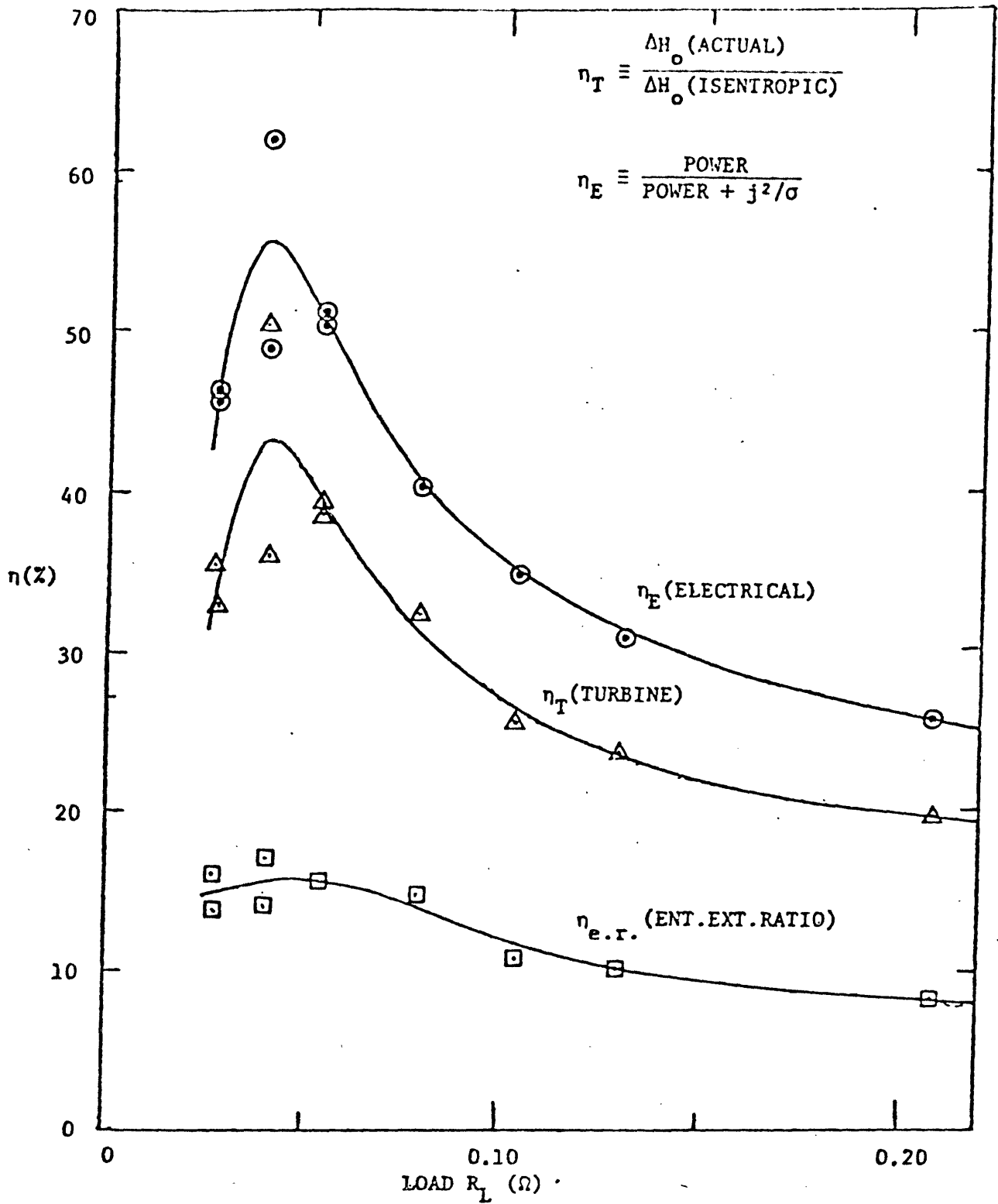
FIGURE 13   EFFICIENCY VS. LOAD: T_o = 3350°K, P_o = 8.0 atm., $\dot{m}$ = 3.7 kg/sec, B = 3.0 T

$$\eta_T \equiv \frac{\Delta H_o \text{(actual)}}{\Delta H_o \text{(isentropic)}}$$

$$\eta_E = \frac{\text{Power}}{\text{Power} + j^2/\sigma}$$

$\eta(\%)$

50

40

30

20

10

0

η_E

η_T

$\eta_{e.r.}$

0   0.05   0.10   0.15   0.20

Load R_L (Ω)
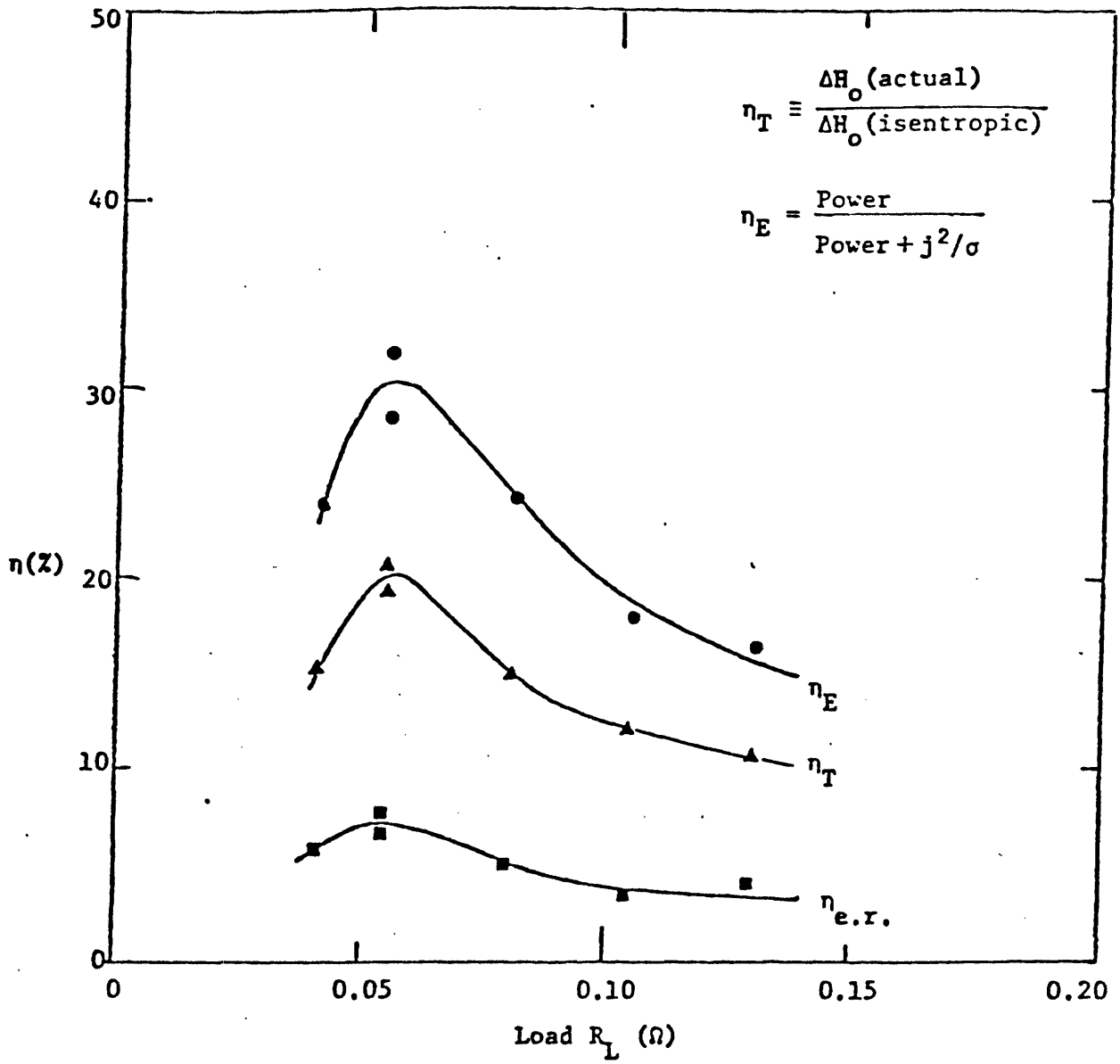
Figure 14   Efficiency vs. Load: $T_o = 2450°K$, $p_o = 6.7$ atm.,
$\dot{m} = 3.7$ kg/sec, $B = 3.0$ T

and $\qquad u = M\sqrt{\gamma RT}$ $\qquad\qquad$ (4)

From static and stagnation pressure measurements, the local Mach number and static temperature are determined from Equations (2) and (3). Since no power is extracted at open circuit, T_0 is nearly constant in the generator. The velocity is then given by Equation (4). E_R is determined from the measured voltage profile in the generator.

The above procedure was used to determine $\omega\tau_{eff}$ for the same stagnation conditions at which the efficiency measurements were made. At $T_0 = 2450K$, values of $\omega\tau_{eff}$ were determined near the generator entrance (upstream of the circular shock) and at the generator exit (see Figure 15). For the $T_0 = 3350K$ cases, $\omega\tau_{eff}$ could only be determined downstream of the circular shock. The efficiency data are compared with the local theoretical results in Figure 16. Good agreement is found between the data and the theory for $K = 1.0$ (45° swirl).

3. Electron Density and Temperature

Electron density and temperature measurements in the generator have recently been initiated. Bifurcated fiber optics are used to obtain a simultaneous observation of the continuum radiation (cesium) in the generator at two wavelengths. The radiation intensity is a function of wavelength, λ, electron density, N_e, and electron temperature, T_e, i.e.,[7]

$$I = f(\lambda, N_e, T_e) \qquad\qquad (5)$$

where I is reduced from a photo multiplier tube output voltage, V_m, which is proportional to the radiation intensity. The electron density and temperature can be determined at a point in the generator from the continuum measurements (V_{m_1}, V_{m_2}) corresponding to radiation at two different wavelengths (λ_1, λ_2).
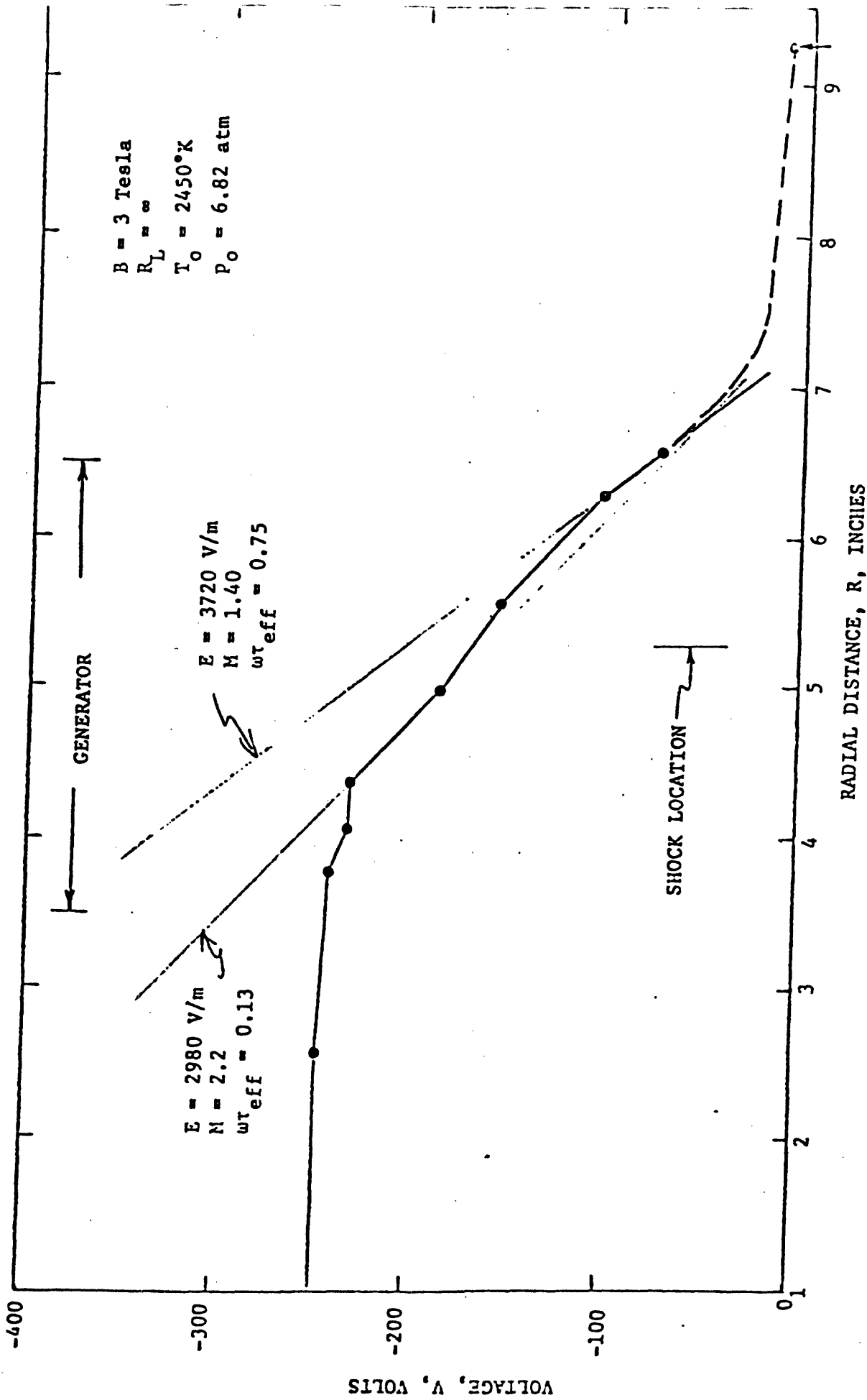
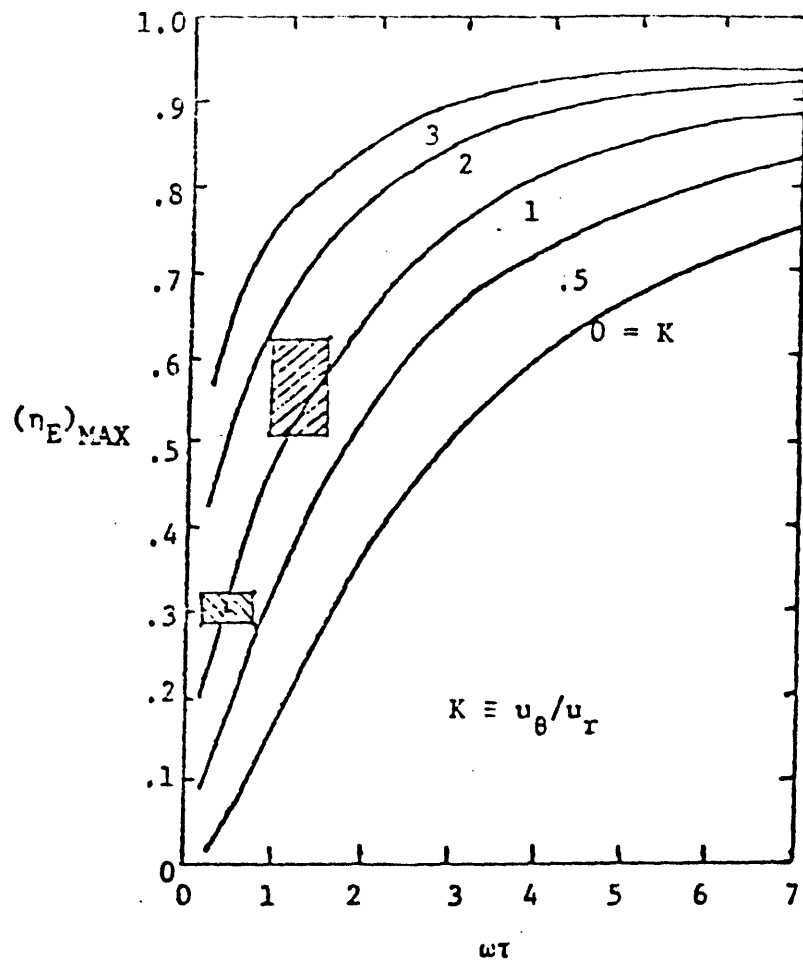Figure 15   Open Circuit Voltage Distribution Used to Determine $\omega\tau_{eff}$

Figure 16　Electrical Efficiency vs.
Swirl Ratio and $\omega\tau$

T_o = 3350°K data

T_o = 2450°K data

The technique is illustrated in Figure 17 for an open-circuit test at T_o = 2450K, p_o = 6.7 atm. Measurements were made at the generator exit (port #5, see Figure 1). The two narrow band filters used were λ_1 = 4907A and λ_2 = 4296A, and corresponding measure voltages were V_{m_1} = 1150 mV and V_{m_2} = 500 mV. Equation (5) is plotted for both sets of values λ, V_m. From the intersection of the two curves, N_e = 3.35x10^{15}cm^{-3} and T_e = 3400K. For these conditions the cesium ionization should be in Saha equilibrium[8]. The dashed curve in Figure 17 are Saha results calculated for T_{gas} = 1500K and p_{cs} = .00275 atm. The gas temperature was determined from static and stagnation pressure measurements and Equations (2) and (3). The cesium partial pressure was determined from the gas static pressure and the seed fraction. For N_e = 3.35x10^{15} cm^{-3}, Saha equilibrium yields T_e = 3500K, in close agreement with the measured results.

The ideal Hall parameter can now be calculated from

$$\omega\tau = \frac{eB}{m_e} \left[\frac{1}{\Sigma(nQ)c_e} \right]$$

where the mean electron thermal velocity,

$$c_e = 1.96 \times 10^5 \left(\frac{T_e}{1000}\right)^{1/2}$$

and $(nQ) = n_a Q_a + (n_{Cs} - N_e) Q_{Cs} + N_e Q_{ei}$.

The following energy-averaged momentum transfer cross-sections are used[7]:

$$Q_a = 0.7 \times 10^{-20} m^2$$

$$Q_{cs} = 400 \times 10^{-20} m^2$$

$$Q_{ei} = 5.85 \times 10^{-10} \ln(1.24 \times 10^7 T_e / N_e) / T_e \ .$$
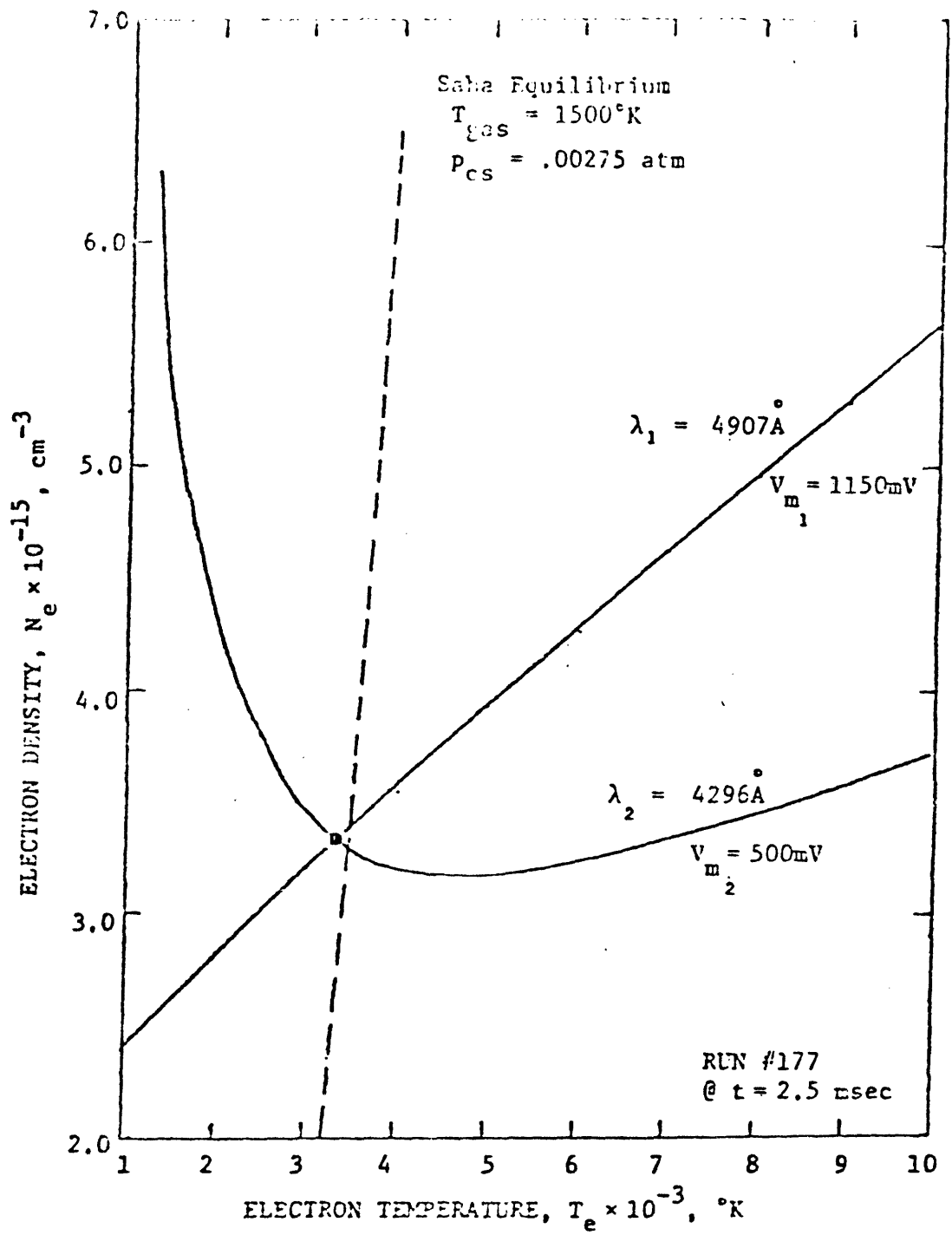
Figure 17   Electron Density and Temperature Measurements
from Continuum Radiation at the Generator Exit.
T_o = 2450°K, p_o = 6.7 atm., B = 3.0 T, R_L = ∞

For the measured values $N_e = 3.35 \times 10^{15} \text{cm}^{-3}$ and $T_e = 3400\text{K}$, we get $\omega\tau = 2.2$. The effective Hall parameter, as determined from open-circuit tests at $T_o = 2450\text{K}$, is 0.75. The effective conductivity can be determined from

$$\sigma_{eff} = \sigma\left(\frac{\omega\tau_{eff}}{\omega\tau}\right) = N_e e \frac{\omega\tau_{eff}}{B}.$$

For $N_e = 3.35 \times 10^{15} \text{cm}^{-3}$, $B = 3.0$ T, and $\omega\tau_{eff} = 0.75$, we obtain $\sigma_{eff} = 135$ mho/m.

E. Conclusions

The performance and interaction physics of a small (volume $\simeq$ 2 liters) nonequilibrium disk generator with 45° inlet swirl has been investigated. Measurements were made of the (a) voltage and static pressure distributions in the generator, (b) stagnation pressure and electron density at the generator exit, and (c) swirl vane and electrode voltages. The generator flow luminosity was recorded with a high-speed framing camera. The significant results and conclusions of this study are as follows:

(1) Power densities from 100 MW/m^3 at 1950K to 500 MW/m^3 at $T_o = 335\text{K}$ (with the corresponding enthalpy extraction range 5% $\leq$ $\eta_{e.r.} \leq$ 15%) were obtained. These results illustrate the enhanced performance of the swirl generator over the performance of both the radial (Hall) generator and a linear Faraday generator. The linear Eindhoven generator provides only about 95 MW/m^3 with an enthalpy extraction of 17% at $T_o = 3300\text{K}$.

(2) A maximum isentropic efficiency of $\eta_T = 51\%$ and a maximum electrical efficiency of $\eta_E = 62\%$ were obtained for $\omega\tau_{eff} \simeq 1.5$. The η_E result is in good agreeement with the local maximum theoretical prediction for 45° swirl and is a factor of two higher than the value predicted for a purely radial flow generator.

(3) The ionization length is short relative to the generator length. Consequently, ionization relaxation does not appreciably affect the generator performance.

(4) As a result of the flow-retarding force $j_\theta B$ (acting radially inward), a shock is present in the generator during the interaction. The shock strength (determined from static pressure measurements) decreases with decreasing load resistance and does not appreciably affect the voltage distribution or the performance of the generator.

(5) Movies of the plasma luminosity clearly reveal (a) the existence of wakes and trailing edge shocks in the generator and (b) the existence of an oblique shock which has good circular symmetry. The position of the shock correlates well with the pressure results in (4) above. The deflection of the wakes through the circular shock shows that the flow remains supersonic and that the swirl angle increases downstream of the shock. No circular shock is observed when the magnetic field is not applied.

(6) The swirl vanes float at the highest potential in the generator plasma, which suggests that no current flows through the vanes. This is an important design consideration for a steady-state generator, since a current concentration at the vane trailing edge would pose a serious materials problem.

(7) Initial results of electron density and temperature measurements near the generator exit confirm that Saha equilibrium exists at the electron temperature.

(8) Performance tests with N_2-CO_2 mixtures are currently underway.

References

1. Louis, J. F., "Disk Generator," _AIAA Journal_, Vol. 6, September 1968.

2. Klepeis, J. E. and J. F. Louis, "The Disk Generator," First U.S./U.S.S.R. Colloquium on MHD Power Generation, Moscow, U.S.S.R., 1974.

3. Hruby, V. J., "Experimental Investigation of the MHD Disk Generator with Inlet Swirl," M.Sc./Engineering Thesis, MIT, February 1976.

4. Louis, J. F., "Research on Inert Gas MHD Conversion," ARL 69-0076, May 1969.

5. Blom, J., et al., "High Power Density Experiments in Eindhoven Shock Tunnel MHD Generator," Proceedings of Sixth International Conference on MHD Electrical Power Generation, Vol. III, Washington, D. C., June 1975.

6. Rosa, R. J., _Magnetohydrodynamic Energy Conversion_, Hill, New York, 1968.

7. Agnew, L. and C. Summers, "Quantitative Spectroscopy of Cesium Plasmas," University of California, Los Alamos Scientific Laboratory, Los Alamos, New Mexico.

8. Kerrebrock, J. L., "Magnetohydrodynamic Generators with Nonequilibrium Ionization," _AIAA Journal_, Vol. 3, April 1965.

COMMENTS ON THE DISK GEOMETRY APPLIED TO
COMMERCIAL CLOSED CYCLE MHD POWER GENERATION

by

James E. Klepeis

Avco-Everett Research Laboratory, Inc.

Everett, Massachusetts

Since October 1976, experimental and analytical disk work at Avco has been oriented toward open cycle rather than closed cycle applications of the geometry. At the present stage of disk development and in terms of commercial application of MHD, it seems clear that the disk channel concept is better suited to the open-cycle case. For the disk to be competitive with linear channels for closed cycle, certain advances have to be made regarding attainable electrical and isentropic efficiency. This subject is discussed below, briefly.

Noble gas shock tube disk experiments, with seeded argon, at Avco and MIT have shown that a closed-cycle disk can achieve high values of enthalpy extraction.[1] Peak values of approximately 17% were reported by both institutions. The Avco disk was a physically large machine using pure radial inlet flow, while the MIT disk was a smaller device (by about a factor of 4) and incorporated inlet guide vanes to provide swirl flow. Nevertheless, the question still remains about a closed-cycle disk's capability to achieve sufficiently high values of electrical and isentropic efficiency. For a commerical MHD plant to operate at an overall efficiency of 50% - plus, corresponding MHD channel isentropic efficiencies are usually in the 70 to 75% range. If the channel is a disk, a requirement exists on the minimum effective Hall parameter, β_{eff}, in order that such isentropic efficiencies be achievable. With inlet swirl flow, the minimum β_{eff} is approximately 4, assuming that one can recover the ideal benefits of swirl with no accompanying harmful effects. In the case of pure radial inlet flow, the minimum β_{eff} required is about 5.5. The difficulty, of course, is that in the closed cycle case, the ionization instability limits the maximum value of β_{eff} to the

range, 1 to 2, namely, far below that required for a disk with or
without inlet swirl. the use of the concept of fully ionized
seed to achieve higher values of β does not seem practical at the
present time. here, one employs either a noble gas temperature
(4000k) that is beyond reach in a practical system; or one uses a
reasonable temperature (2000k), but at seed fractions so tiny as
to yield unacceptably low values of plasma electrical conduc-
tivity. it seems, therefore, that in order for the disk to be
competitive in closed cycle applications, some other mechanism
must be found that will allow higher values of β_{eff} to be
attained. for open cycle disks, the situation is quite different
since β_{eff} of 5 and greater have been experimentally observed.[2]

References

1. Proc. of the 15th Symposium on the Engineering Aspects of
    MHD; papers by J. Klepeis, et al (AVCO) and J. Louis, et al
    (MIT); U. of PA, PA. (1976).

2. Klepeis, J. and Louis, J. "Research on MHD Energy
    Conversion", ARL Report No. 70-0244, WPAFB, Dayton, Ohio
    (1970).

THE DISK GENERATOR PROGRAM AT STANFORD

by

Takashi Nakamura

Department of Mechanical Engineering

Stanford University

Stanford, California

Construction of a small-scale combustion-driven disk genera-
tor experimental facility is in progress at Stanford. The typi-
cal dimension and the characteristics of the generator are as
follows:

disk inner diameter	5 cm
disk outer diameter	15 cm
mass flow rate (alcohol + N_2/O_2)	0.1 ≃ 0.2 kg/s
magnetic field	6 T

The apparatus is currently undergoing a series of thermal
tests for thermal and electrical insulation.

It is important to compare the predicted performance charac-
teristics of the Stanford Disk Generator with those of previously
conducted experiments elsewhere. Such a comparison is helpful in
defining the direction in which future research efforts are to be
oriented.

In Figure 1 the electrical characteristics of the various
disk generators are shown. Each data point represents the open-
circuit electric field and the short-circuit current density
$I_s/2\pi\, r_e\, z_e$, where I_s is the short-circuit current and r_e and z_e
are the radius and the width of the generator at the exit, respec-
tively. With the exception of the blow-down experiments[3] all the
experiments have been conducted with a shock-tube facility using
alkali-seeded noble gas[4,6,7,8] or alkali-seeded molecular
gas.[5,9,10] The predicted electrical characteristic of the
Stanford Disk Generator[11] will be compared to that of the AVCO
Large Disk operating with simulated combustion gases.[9,10] An
electric field of more than 10 kV/m, the value expected for

commercial disk generators, will be achieved.

Figure 2 shows the enthalpy extraction characteristic of various disk generators. Enthalpy extraction is plotted against $L/L_{E.E.}$, where L is the generator length $(r_e - r_i)$ and $L_{E.E.} = (\rho\ h_{tot}/\sigma\ v_r\ B^2)i$ is a characteristic length for enthalpy extraction where the density ρ, conductivity σ, and radial velocity v_r are evaluated at the inlet of the disk generator. In contrast to the MIT shock-tube experiment[7] or the AVCO large shock-tube experiment[8] for which high enthalpy extraction was made possible due to high electrical conductivity ($^\sim 10^2$ mho/m) and large generator size (L = 36 cm for AVCO large disk), the enthalpy extraction of the Stanford Disk Generator is limited to less than 1% because of its small size (L = 5 cm) and relatively low electrical conductivity ($^\sim 10$ mho/m).

The results of the disk generator survey presented above show that although the Stanford Disk Generator Facility's small scale yields a limited enthalpy extraction, it will provide crucial information concerning the electrical characteristics of the full-scale, central-station disk generator.
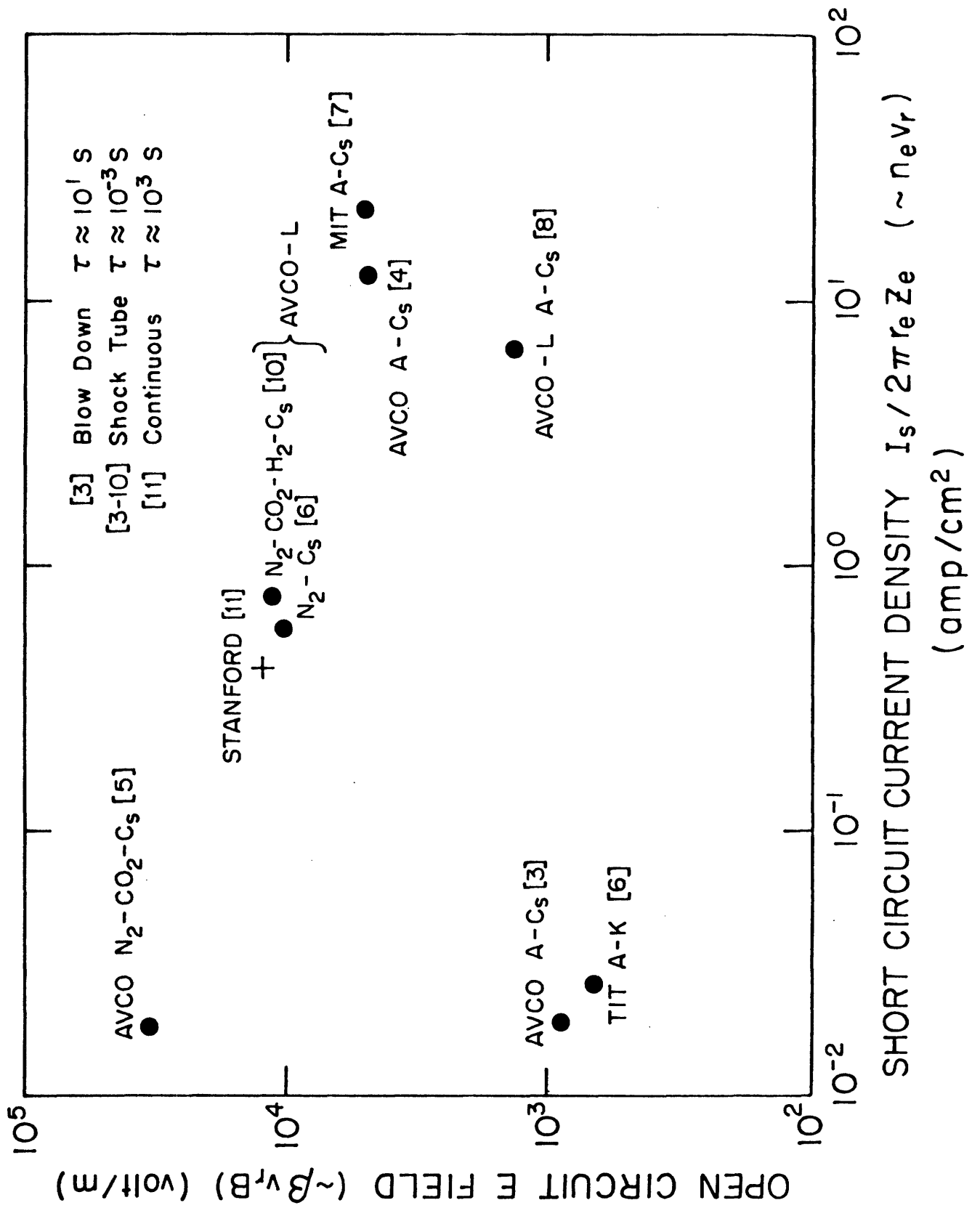
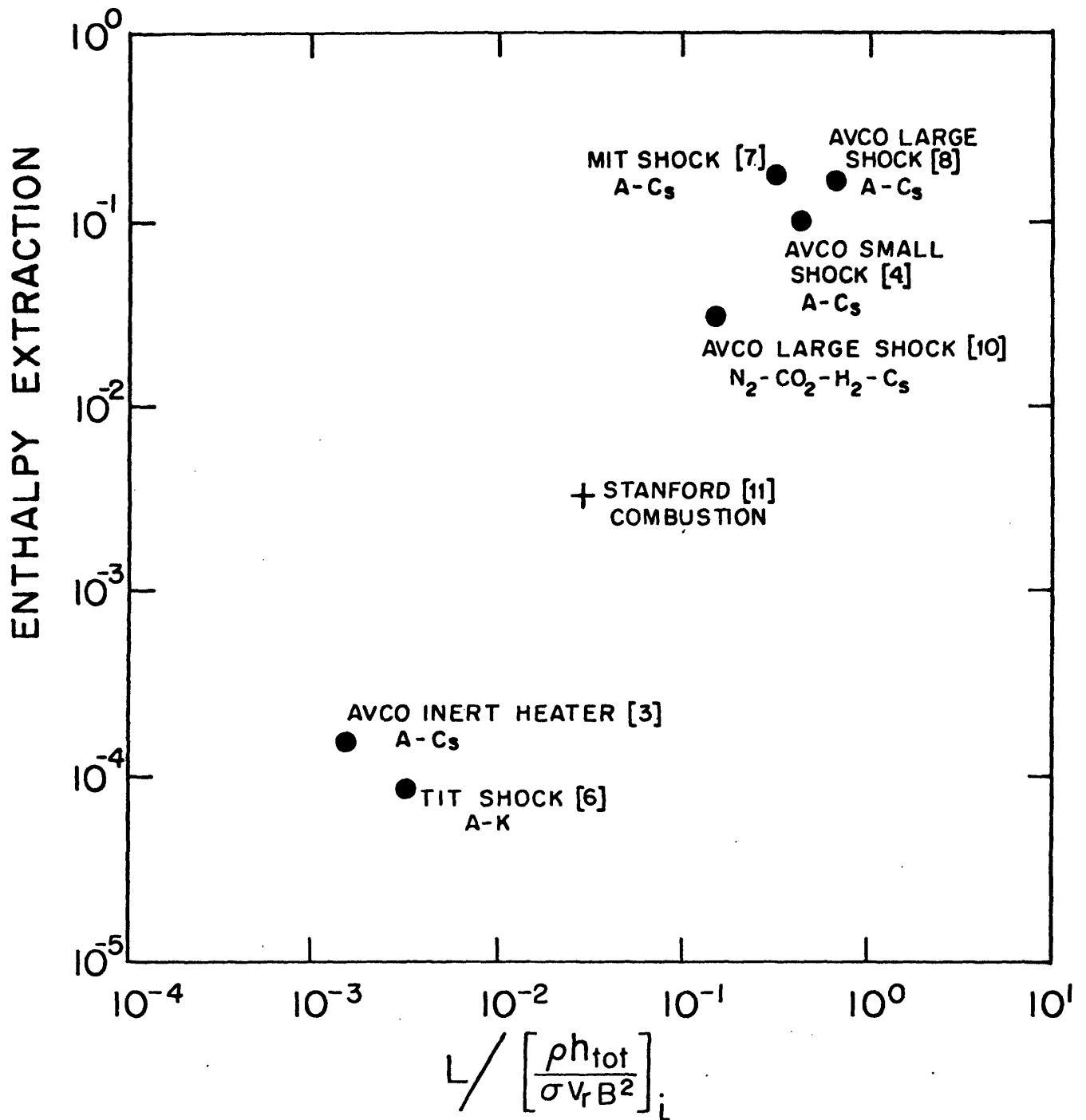Figure 1. Electrical Characteristics of Various Disk Generators.

Figure 2. Enthalpy Extraction of Various Disk Generators

REFERENCES

[1] [2] do not appear in this summary write-up.

[3] Klepeis, J., and Rosa, R. J., "Experimental Studies of Strong Hall Effects and $\vec{V} \times \vec{B}$ Induced Ionization," 5th Symposium on Engineering Aspects of Magnetohydrodynamics, MIT, April 1964 and Klepeis, J. and Rosa, R. J., "Experimental Studies of Strong Hall Effects and $\vec{U} \times \vec{B}$ Ionization - II," 6th Symposium on Engineering Aspects of Magnetohydrodynamics, Pittsburgh, April 1965.

[4] Louis, J. F., "Studies on an Inert Gas Disk Hall Generator Driven in a Shock Tunnel," 8th Symposium on Engineering Aspects of Magnetohydrodynamics Stanford, March 1967.

[5] Klepeis, J. E. and Louis, J. F., "High Hall Coefficient Studies in a Disk Generator Driven by Molecular Gases," 10th Symposium on Engineering Aspects of Magnetohydrodynamics, MIT, March, 1969; and Klepeis, J. E. and Louis, J. R., "Studies with a Disk Generator Driven by Molecular Gases," 11th Symposium on Engineering Aspects of MHD, Pasadena, March 1970.

[6] Shioda, S. and Yamasaki, H., "Generation Experiments with a Disk MHD Generator Under the Conditions of Fully Ionized Seed," 6th International Conference on Magnetohydrodynamic Electrical Power Generation, Washington, D.C., June 1975.

[7] Loubsky, W. J., Hruby, V. J., and Louis, J. F., "Detailed Studies in a Disk Generator with Inlet Swirl Driven by Argon," 15th Symposium on Engineering Aspects of Magnetohydrodynamics, Philadelphia, May 1976.

[8], [9] Klepeis, J. and V. Hruby, "MHD Power Generation Experiments with a Large Disk Channel: Verification of Disk Scaling Laws," 15th Symposium on Engineering Aspects of Magnetohydrodynamics, Philadelphia, May 1976.

[10] Klepeis, J. and Hruby, V., "The Disk Geometry Applied to Open Cycle MHD Power Generation: Theoretical Considerations & Experiments," 16th Symposium on Engineering Aspects of Magnetohydrodynamics, Chicago, May 1977.

[11] "A High Magnetic Field MHD Generator Program, Part II - Technical Proposal," High Temperature Gasdynamics Laboratory, Stanford University, May 1976.

PLASMA PHENOMENA

SUMMARY: ELECTRIC SHEATH CHARACTERISTICS ON MHD ELECTRODES

by

H. K. Messerle
University of Sydney
Sydney, Australia

The gaseous boundary layer of an electrode in an MHD gener-
ator is made up of three components: the gas dynamic layer, the
thermal layer and the electrostatic sheath. They can be influ-
enced quite critically by the surface through its chemical con-
stitution, its surface topology and temperature.

The work here deals primarily with the gaseous phase and
assumes a perfectly flat surface with varying temperature, but
allowing for no thermionic emission. Layer studies in the past
have assumed normally a constant temperature across the layer.
In an MHD generator, the wall temperature seems to be well below
that of the bulk plasma, hence, a temperature layer with a steep
temperature gradient as the electrodes develop. This temperature
layer has the same order of thickness as the fluid dynamic layer
under usual operating conditions in an MHD duct. The elec-
trostatic layer has been assumed normally to be much thinner and
well below 0.1 mm thickness.

Under the condition considered here, the electrostatic layer
is shown to expand as voltage and current across a duct rises; and
it extends right to the edge of the thermal layer until it col-
lapses because of localized electrostatic breakdown.

To show this, a simple layer model was developed (Figure 1).
Inside the bulk plasma an even ion and electron distribution is
assumed to be established as determined by thermionic equilibrium
conditions. In the cathodic electrostatic layer the current is
transferred by the ions, where the electrons are being withdrawn
into the plasma. The model assumes a step transition from ionic
to electronic current at the plasma edge. Without going into
further detail, the mathematical analysis leads to a collisional
ionic electrostatic layer. The results had two sets of
characteristic voltage: current relations from which conditions

for electrostatic breakdown and arc spot formation can be deduced. The results tie in with experimental data obtained on an arc torch-driven experimental facility.

Further, work has commenced using a more detailed continuity equations for electrons and ions in the layer region. This work has confirmed the use of the simplified model at least for situations in which we are dealing with thin thermal boundary layers.

# NONUNIFORMITIES IN MHD PLASMAS AND REDUCTION

FORMULAE FOR OHM'S LAW

by

S. E. Shamma, M. Martinez-Sanchez, and J. F. Louis

Massachusetts Institute of Technology

Cambridge, Massachusetts 02139

Small scale inhomogeneities of the transport properties of unbounded plasmas are known to have a strong effect on their macroscopic current properties, especially at high values of the Hall parameter, β.[1,2,3] The performance of MHD generators, which is critically dependent on favorable values of these properties, is, therefore, affected by sources of inhomogeneity, such as incomplete molecular scale mixing of seed and gas, and of hotter and colder gas regions. Very few exact solutions are known for the effective Ohm's law of inhomogeneous plasmas. The best known being that for a layered medium,[1] which first displayed clearly the strong effect of the Hall parameter. Other solutions are for a two-dimensional symmetric plasma,[3,6] as well as the limiting cases[4] of "dilute suspensions" of possibly strong inhomogeneities, and of isotropic inhomogeneities with small amplitude.[2,7]

We report here the results of our recent investigation[5] of several types of anisotropic inhomogeneities, including "streamers" in the plane orthogonal to the magnetic field $\vec{B}$, and plasmas with isotropy in that same plane, but with different degrees of ellipticity along the $\vec{B}$ direction. Two methods were used: (a) an extension of the small perturbation technique to anisotropic cases; (b) an approximate "self-consistency" method devised to extend the range of validity of (a) to high β and strong inhomogeneities.
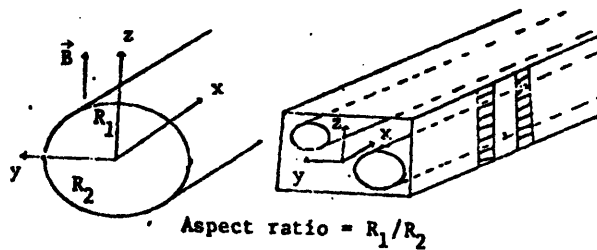
Aspect Ratio = R_1/R_2

Figure 1. Plasma with "streamers", i.e., with constant properties in a certain direction normal to $\vec{B}$, but with nonuniformities in the transverse plane (which contains $\vec{B}$).
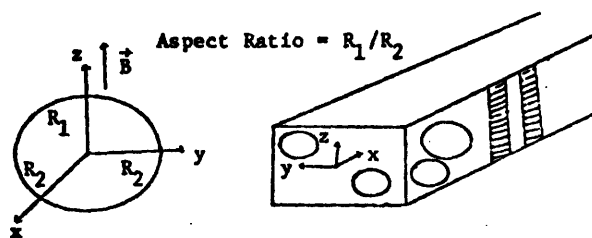
Aspect Ratio = R_1/R_2

Figure 2. Plasma with nonuniformities which are isotropic in the x-y plane, but either shortened or elongated along the magnetic field.

Both methods are found to agree well when the fluctuations are weak, but differences appear at high fluctuation levels, and for nonuniformities very elongated along $\vec{B}$, also when the Hall parameter β is high. Comparison with available exact solutions[3,6] valid at high β and strong fluctuations and results for some limiting cases,[1,4] indicate that the self-consistency method gives accurate results in these cases.

The results of these analyses are used to evaluate the performance reduction in MHD channels with plasma nonuniformities of several geometries, including axial streamers, perfectly isotropic fluctuations, and fluctuations elongated along $\vec{B}$; the power density is reduced most strongly when β and the r.m.s. of the fluctuations are high, and also when the inhomogeneities are stretched along the magnetic field.

References

1. Rosa, R. J., "The Hall and Ion Slip Effects in a Nonuniform Gas," Physics of Fluids, 5, No. 9, pp. 1081-1090 (1962).

2. Yoshikawa, S., and D. J. Rose, "Anomalous Diffusion of a Plasma Across a Magnetic Field," Physics of Fluids, 5, No. 3, pp. 334-340 (1962).

3. Martinez-Sanchez, M., R. DeSaro and J. F. Louis, Effective Ohm's Law for a Class of Inhomogeneous Plasmas, and its Effect on the Performance of Combustion-Driven MHD Generators," Proceedings of the Sixth International Conference MHD Generation, Vol. 4, pp. 247-264, Washington (1975).

4. Emets, Y. U., A. P. Rasheheskin, V. F. Reagtsov and A. K. Shidlovskiy, "Electrodynamic Problems and Electrical Parameter Stabilization Methods in MHD Generators with Nonuniform Flow," Ibid, pp. 203-215.

5. Shamma, S. E., M. Martinez-Sanchez and J. F. Louis, "Ohm's Law for Plasmas with Non-Isotropic Inhomogeneities and Its Effects on the Performance of MHD Generators," Sixteenth Symposium on Engineering Aspects of MHD, pp. VII.1.1-7, Pittsburgh, Pa., May (1977).

6. Dykne, A. M., "Anomalous Plasma Resistance in a Strong Magnetic Field," Soviet Physics JETP, 32, No. 2, February (1971).

7. Louis, J. F., "Effective Ohm's Law in a Partially Ionized Plasma with Electron Density Fluctuations," Physics of Fluids, 5, No. 9, pp. 2062-2064 (1967).

A STATISTICAL APPROACH IN TIME SERIES FLUCTUATION ANALYSIS OF ELECTRON TEMPERATURE AND ELECTRON DENSITY IN AN MHD GENERATOR

by

A. A. Jongbloed and W. M. Hellebrekers

Eindhoven University of Technology, Netherlands

1. Introduction

From the radiation energy due to electron-Cs^+ recombinations in a cesium-seeded noble-gas MHD generator information is obtained about the behavior of electron temperature and electron density.

After sampling the radiation energy signals at two wavelengths during 1 msec in experiments with a shock tunnel facility, two 1000-samples sequences are generated: one is the temperature sequence T_e; the other gives its density N_e.

In order to investigate the presence of a possible relation between T_e and N_e, some statistical correlation properties are the topic of observation here.

2. Frequency Distributions and the Saha Equilibrium

As is done in previous work, two separate frequency distributions f_T and f_N can be made by counting the events T_e and N_e, respectively, falling within a certain number of classes. In order to discover whether a two-dimensional simultaneous frequency distribution f_{NT} could affirm a relation $N_e = N_e(T_e)$ or not, this simultaneous distribution has been investigated for several runs. By counting the events in the T_e-N_e sequence that the couple (T_e, N_e) lies in a certain two-dimensional class, we obtain such a discrete simultaneous frequency distribution f_{NT} as a matrix, see Figure 1. Summing rows in this matrix gives the distribution f_N; by summing the columns, the one-dimensional distribution f_T is obtained. For all runs observed, no specific orientation in the distribution f_{NT} has been found. This is in

accordance with estimation results for the correlation coefficient r: $|r| < 0.1$, which are values such as to reject a hypothesis about significant correlation between N_e and T_e.

With respect to a relation $N_e = N_e(T_e)$ supposed, the orientation should be the slope of the linear regression:

$$\hat{N}_e = aT_e + b$$

slope: $a = r\, s_N/s_T$ r: correlation coefficient

s_N: spread in N_e

s_T: spread in T_e (see Table 1)

If an equilibrium (Saha) does exist in ionization and recombination of the seed, this yields a relation $N_e = N_e(T_e)$ as is illustrated in Figure 2. The slope occurring at 0.03% seeded argon is about $4/1000 \times 10^{20}$; with the found values for s_N and s_T the found $r \simeq 0$ does not affirm this equilibrium. A slightly seeded argon could maintain the postulation of such an equilibrium, but the low N_e saturation value in that case would exclude electron densities as found in experiments (9×10^{20} m^{-3} max). Experimental density values give as a minimum value a 0.03% seeded argon; this minimum, furthermore, rejects the presence of the Saha equilibrium for mean values $\langle T_e \rangle$ and $\langle N_e \rangle$ (Table 1) and for low-frequency fluctuations (determined by averaging 100 µsec blocks) as shown in Figure 3 and Figure 4.

The conclusion is that the Saha equilibrium exists, neither in fast fluctuations, nor in slow ones.

The uncorrelated behavior in N_e and T_e is the main reason for the issue of statistical independence to be made in all the following calculations. When results obtained with f_{NT} are compared with results from both f_N and f_T, no significant difference has been found. Therefore, two-dimensional simultaneous frequency distributions have no further use: the needed statistics will be extracted from the distribution f_N and f_T.

3. Mean Values of Conductivity and Hall Parameter

both: Conductivity σ and Hall parameter β depend on t_e and N_e

$$\text{conductivity:} \quad \sigma = \frac{N_{e*} \, e^2}{m_e^* \, (\bar{\nu}_{ei} + \bar{\nu}_{eh})}$$

$$\text{Hall Parameter:} \quad \beta = \frac{e*b}{m_{e*} \, (\bar{\nu}_{ei} + \bar{\nu}_{eh})}$$

e: electron charge
m_e: electron mass
B: magnetic induction
$\bar{\nu}_{ei}$: mean collision frequency electrons - ions
$\bar{\nu}_{eh}$: mean collision frequency electrons - heavy particles

$$\bar{\nu}_{ei} = 3.64 \times 10^{-6} \times \frac{N_e}{T_e^{3/2}} \ln \left\{ 1.24 \times 10^7 \times \left(\frac{T_e^3}{N_e}\right)^{1/2} \right\}$$

$$\bar{\nu}_{eh} = N_{ar} \times 1.5525 \times 10^{-17} \times T_e^{1/2} \times \exp\,(T_e/T_1)$$

N_{ar}: argon density
T_1: 2200 K

Mean values and variances are estimated with:

$$\langle \sigma \rangle = 1/N^2 \sum_{i=1}^{k} \sum_{j=1}^{k} \sigma(i,j) \times f_N(i) \times f_T(j)$$

$$s_\sigma^2 = 1/N^2 \sum_{i=1}^{k} \sum_{j=1}^{k} \sigma^2(i,j) \times f_N(i) \times f_T(j) - (\langle \sigma \rangle)^2$$

$\sigma(i,j)$ is the value for $\sigma(N_e, T_e)$ after the mean value of class i in the N_e - distribution f_N and of class j in the T_e distribution f_T have been substituted. N is the number of samples, k the number of classes. In an analogous way $\langle\beta\rangle$ and s_β^2 are obtained, and also $\langle g\rangle$ and s_g^2 of any function $g = g(N_e, T_e)$.

With $\langle\sigma\rangle$ and $\langle\beta\rangle$, the reduction factor (cf. ref.) R can be found, after $\rho = (1 + \beta^2)/\sigma$ has been averaged:

$$R = \frac{1}{\sqrt{\langle\rho\rangle\langle\sigma\rangle - \langle\beta\rangle^2}}$$

Estimation results for means and variances and the reduction factors are tabulated in Table 2.

4. <u>Autocorrelation and Cross-Correlation</u>

Up to this moment, dynamic aspects were not the topic of discussions: the frequency distributions f_N and f_T do not maintain the time sequence in the original data series.

Now that a relation $N_e = N_e(T_e)$ is contradicted by correlation results as mentioned before, dynamic properties of correlation in both T_e and N_e sequences are investigated. Estimations $R_{TT}(\tau)$ and $R_{NN}(\tau)$ for autocorrelations of T_e-N_e respectively, cross-correlations are found by determining correlation coefficients after the sequence indicated when the first subscript has been shifted over τ events. In the cross-correlation case, we have, for instance, the derived sequences:

$$T_e(1), \; T_e(2), \; \ldots\ldots, \; T_e(N-\tau)$$
$$N_e(1+\tau), \; Ne(2+\tau), \; \ldots\ldots, \; N_e(N)$$

The loss of 2τ data couples limits the shift τ for reasons of acccuracy:

$$\tau \leq 1/4N$$

Note: The original data T_e and N_e are correlated for non-stationarity (slow fluctuations) in the behavior of the mean temperature and density (see Figure 3 and Figure 4).

In this way, results as shown for run 1735 in Figures 5, 6, and 7 are found. The other runs have the same behavior.

The properties of the correlation functions shown only can be explained using a suitable identification model obtained from fluctuation theory. Without such a model, some phenomena are, however, worthy of mention.

a. The behavior of R_{TT} indicates the presence of undamped oscillations in T_e.

b. Time constants are estimated by fitting models like:
$$\hat{R}_{TT}(\tau) \approx (\beta + \lambda e^{-\sigma\tau}) \cos 2\pi f\tau$$

This yields for run 1735:

$\beta = 0.1$ $\qquad\qquad\qquad\qquad \alpha = 28 \times 10^4 \ sec^{-1}$

$\lambda = 0.9$

$f = 67 \ kHz$ $\qquad\qquad\qquad {}^\tau T_e = 1/\alpha = 3.6 \ \mu sec$

$$\hat{R}_{NN}(\tau) \approx \lambda e^{-\alpha\tau} \cos 2\pi f_1\tau + \beta \cos 2\pi f_2\tau$$
$\beta = 0.15$

$\lambda = 0.85$ $\qquad\qquad\qquad \alpha = 10.5 \times 10^4 \ sec^{-1}$

$f_1 = 33 \ kHz$

$f_2 = 67 \ kHz$ $\qquad\qquad\qquad {}^\tau N_e = 1/\alpha = 9.5 \ \mu sec$

Other runs show the same ratio in ${}^\tau T_e$ and ${}^\tau N_e$:
the time constant for N_e is about twice the value in the T_e case,
$${}^\tau N_e \approx 2{}^\tau T_e$$

c. The cross-correlation behavior as shown in Figure 7 should not be identified here: it depends on the chosen class (linear or nonlinear) of models to be identified. This could be the topic of further investigations.

References

Hellebrekers, W.M., A. Veefkind, et al., "Experimental Fluctuation Analysis in a Noble Gas MHD Generator. (To be presented at the 16th Symposium Engineering Aspects of MHD, May 1977, University of Pittsburgh).

Table 1

run	$\langle T_e \rangle$	s_{T_e}	$\langle N_e \rangle$	s_{N_e}
1735	3665	509	4.23	1.3
1737	3572	375	5.14	1.4
1739	3692	493	4.74	1.2
1740	3508	376	5.27	1.3
1741	3559	334	5.56	1.2
1742	3555	405	3.88	1.0
1743	3637	370	5.74	1.6
1744	3633	297	6.36	1.4

Table 2

run	$\langle \sigma \rangle$	s_σ	$\langle \beta \rangle$	s_β	$\langle \rho \rangle$	R
1735	210	31	6.98	1.2	0.26	0.41
1737	233	24	6.20	1.0	0.18	0.53
1739	224	26	5.83	1.0	0.17	0.49
1740	234	22	5.22	1.0	0.13	0.55
1741	241	20	6.43	0.8	0.18	0.70
1742	207	25	4.86	1.0	0.13	0.55
1743	242	25	8.04	1.0	0.30	0.36
1744	256	21	7.25	0.8	0.22	0.51

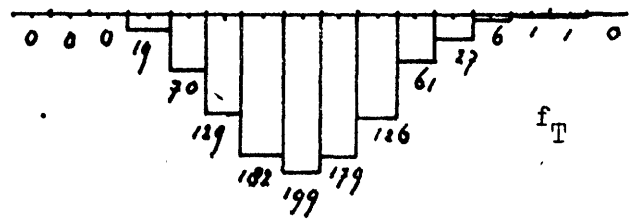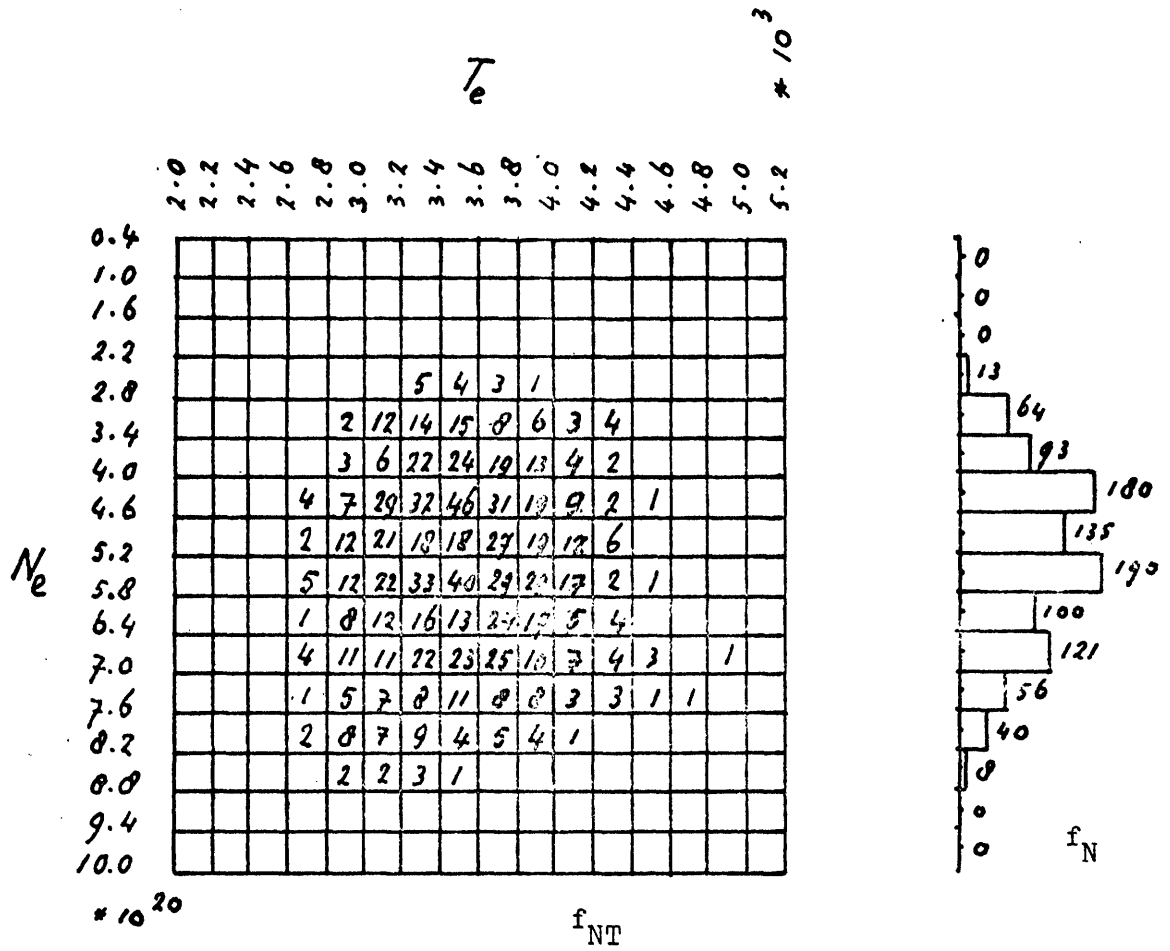T_e $* 10^3$

N_e

f_{NT}

$* 10^{20}$

f_N

f_T

fig.1

f_{NT}, f_N and f_T for run 1740.

Window for T_e: 200

Window for N_e: $0.6 * 10^{20}$

Number of samples: 1000

(Temperatures in K, densities in m^{-3})

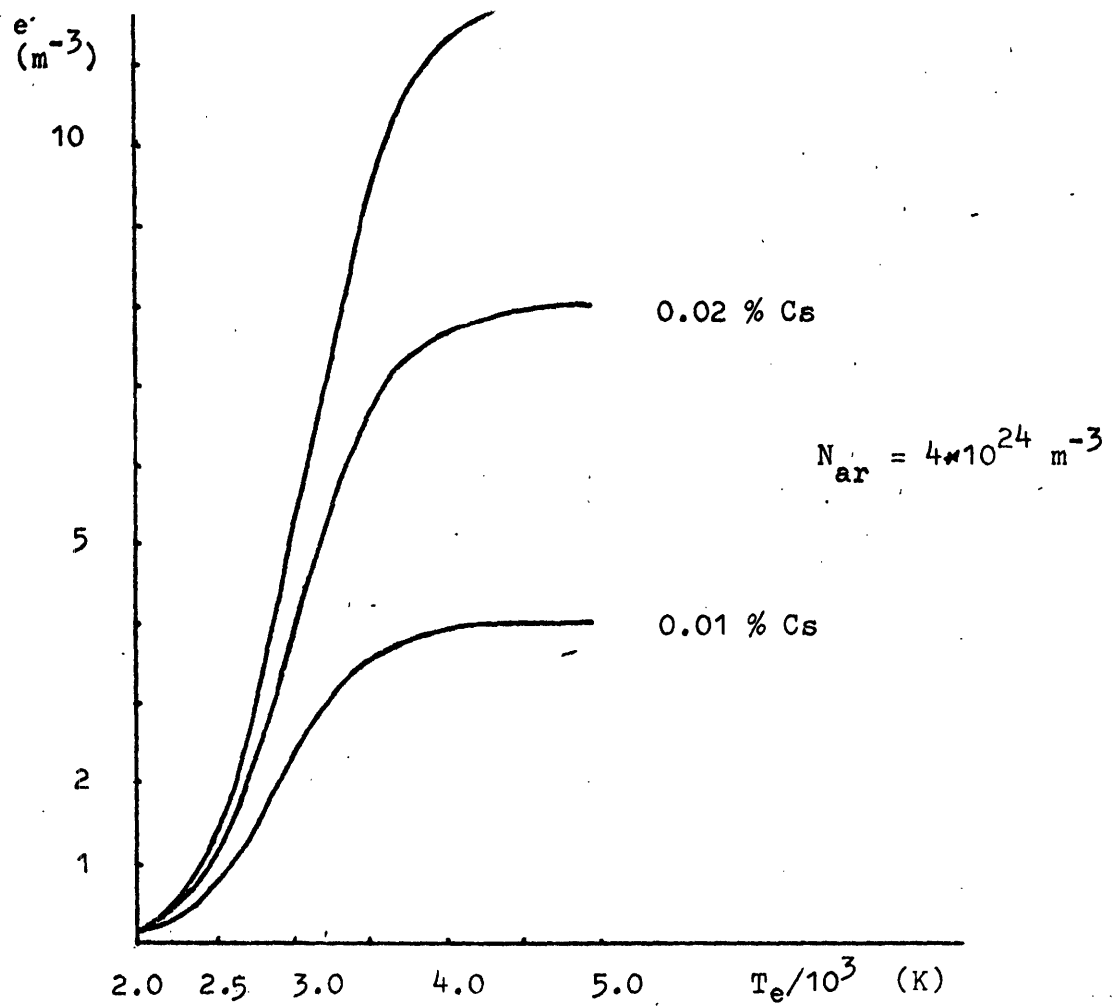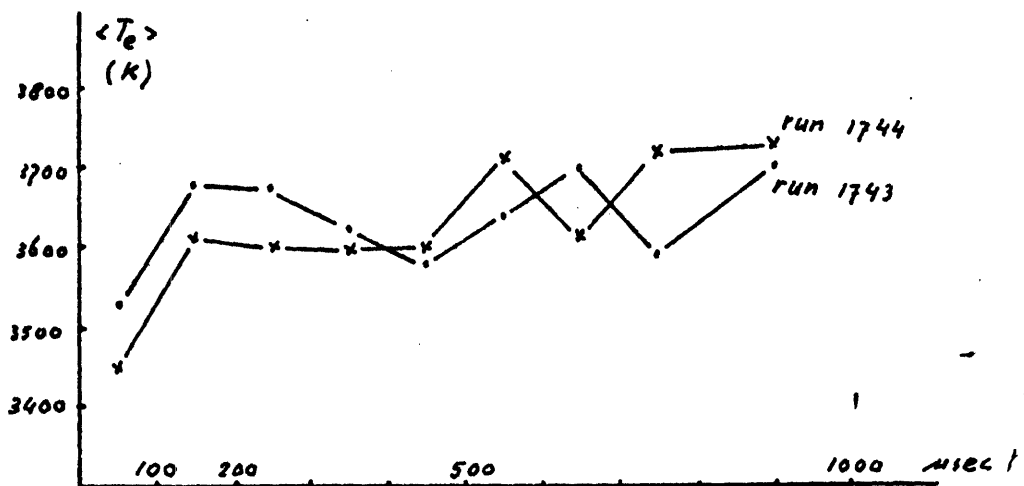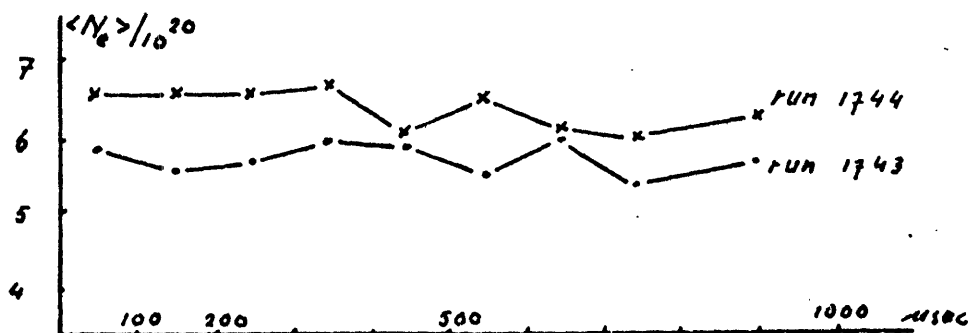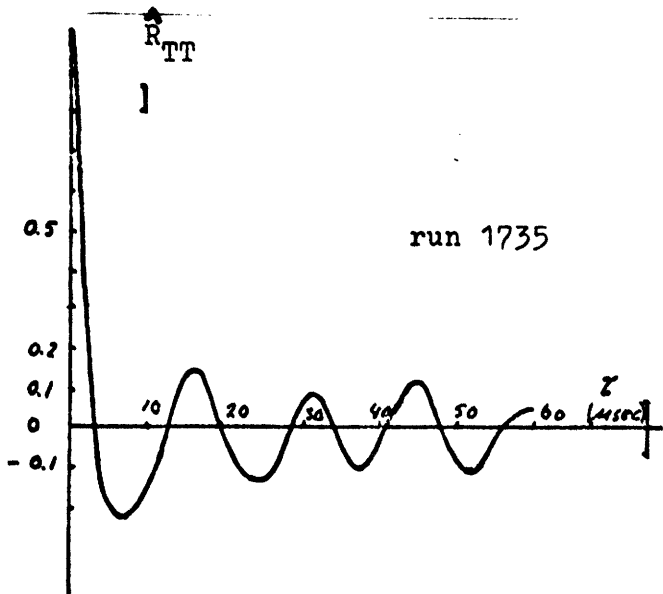fig.2

fig.3

fig.4

fig.5
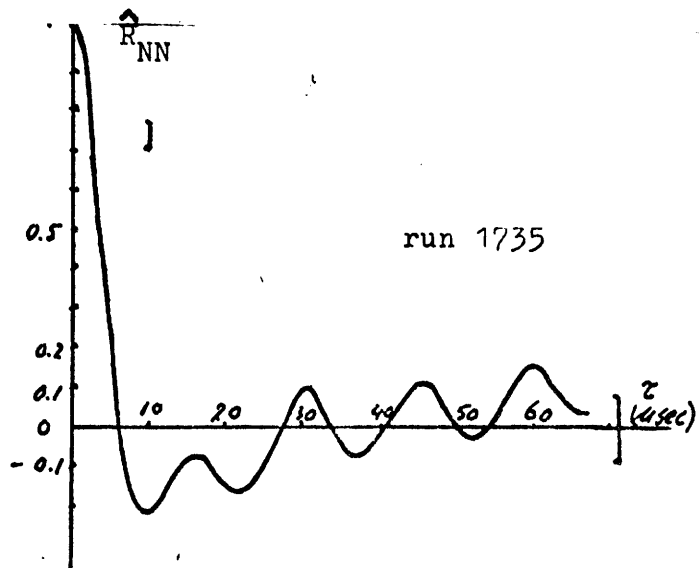
fig.6
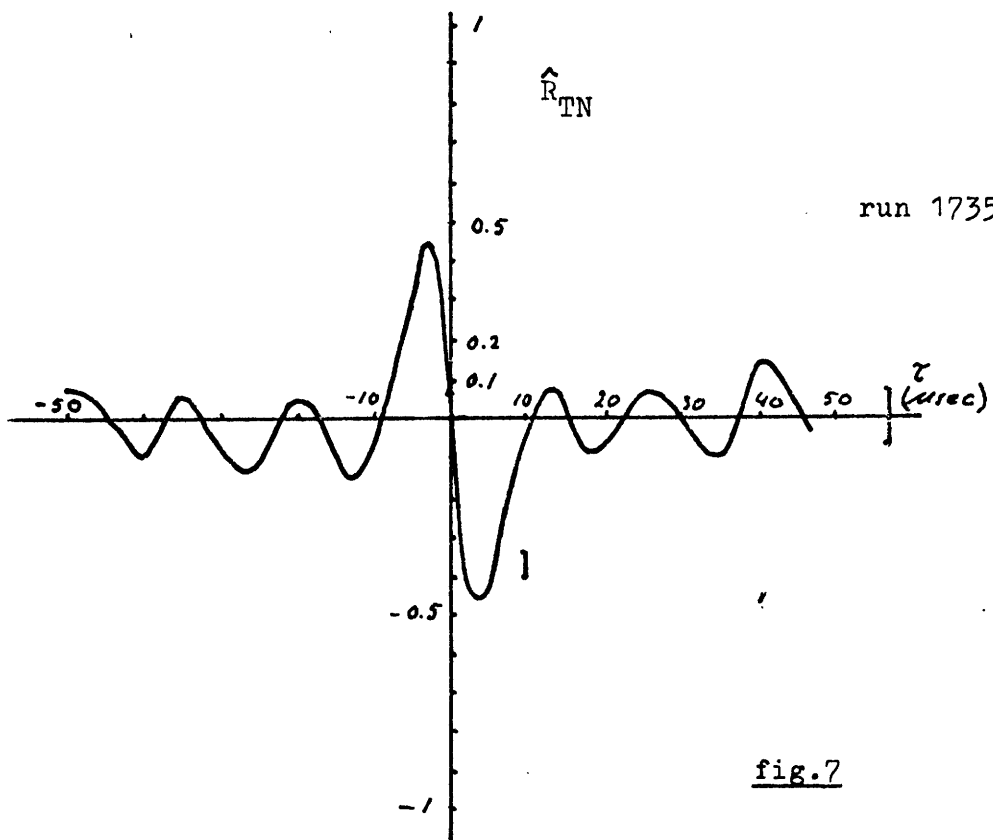
fig.7

Acknowledgements

CLOSED CYCLE MHD

RESEARCH AT GENERAL ELECTRIC COMPANY

by

Charles H. Marston

General Electric Company

Philadelphia, Pennsylvania

A multi-faceted ERDA-funded program is in progress at
General Electric Co., Space Sciences Laboratory for assessing the
feasibility of direct coal-fired Closed Cycle MHD power genera-
tion. Three tasks have been defined:

Task I — Evaluation of argon working fluid contamina-
tion by combustion gas in a ceramic regener-
ative heat exchanger.

Task II — Conversion of the heat exchanger to direct
coal firing.

Task III — Analytical support.

The first task has been completed and has been reported on
in detail by Cook and Dickinson.[1] Contaminant levels after 80
free volumes of argon flow (vs. approximately 500 for a complete
blowdown half-cycle) are well below 10 ppm for CO_2 and no greater
than the <100 ppm detection threshold for N_2 and H_2O. Water
vapor, which had been at saturation (several thousand ppm) was
reduced to its expected level after elimination of condensate
trapped in the system and an increase in the closed-loop cooling
water temperature to just above the system dew point.

Particulate measurements were made using both laser light
scattering and a photometric technique, and some preliminary re-
sults were obtained on the effect of fly ash. The fly ash was
injected for about three hours and resulted in a penetration of
about 1/2 inch into the top bricks. No evidence of deposition
along the flow passages was observed until well below the solidi-
fication temperature. At a level corresponding to $1000^\circ F$, some
loosely adhering slag was observed. Additional work is planned
for fly ash injection over a sufficiently long time to approach a
steady state.

On disassembly of the bed, a few isolated web fractures in the axial direction were observed in the bricks located at the matrix height corresponding to maximum thermal stress, but no functional failure occurred.

Design of the combustor to be used for direct coal firing of the heat exchanger, Task II, is essentially complete and modification of the facility has begun. Design maximum temperature will be 3600°F, which makes possible a distinctly different approach from that necessary for open-cycle MHD coal combustors. The combustor will be a single-stage horizontal cyclone with axial swirl injection. The ceramic lining will be air cooled with the internal surface designed to operate at a slag fusion temperature. Air cooling will permit adjustment of wall temperature over a range from 2300°F to 2700°F. Combustion air will be preheated separately for experiment flexibility, but the design is easily adapted to use of the coolant air for this purpose to minimize combustor heat loss.

In addition to support of the experimental and design activities summarized above, analytical effort has been focused in two areas: 1) the effect of molecular contaminants on non-equilibrium MHD generator performance, and 2) extension of the ECAS Phase 1 CCMHD system studies to a depth comparable to that given Open Cycle MHD in ECAS Phase 2. The contaminant work is discussed by Dellinger in a separate summary, while the system work has been reported on in detail by Marston, et al.[2] at the recent 16th EAMHD Symposium, and a brief summary is given below.

A 1000 MWe coal-fired plant with a steam bottoming plant was studied. The plant incorporates a two stage, 10 atmosphere, fluidized bed combustion system, which meets all emission control requirements. A coal-to-bus bar efficiency of 47% was calculated. This result is essentially the same as that for ECAS case 102A (4 atm combustion pressure) though there were several significant differences in detail. Operating temperatures are rather tightly fixed at 3350°F flame temperature, 3300°F maximum ceramic temperature, 3000°F argon temperature by a combination of material, emission and generator performance constraints. The

steady-state performance of the heat exchanger system has been analyzed and a DC-DC conversion system worked out for economical utilization of a Faraday-connected linear MHD generator. Plant layouts have also been prepaid and costing for both pressurized and atmospheric combustion plants is now in process.

References

1. Cook, C. S. and Dickinson, K., 16th Engineering Aspects of MHD Symposium, Pittsburgh, Pa., May 1977, II.4.

2. Marston, C. H., et al., 16th Engineering Aspects of MHD Symposium, Pittsburgh, Pa., May 1977, X.5.

SUMMARY:
CLOSED CYCLE MHD RESEARCH AT TOKYO INSTITUTE OF TECHNOLOGY

by

Susumu Shioda

Tokyo Institute of Technology

Tokyo, Japan

Current and planned closed cycle MHD programs at Tokyo Institute of Technology consist of the following items:

1. Demonstration of recovery of σ_{eff} and β_{eff} in both disk and linear generators due to suppression of ionization instability.

2. Extraction of large power density at high loading factor with a small seed fraction ($\sim 10^{-5}$).

3. Investigation of effects of molecules on electron temperature and suppression of ionization instability.

4. Investigation of mutual interactions between discharge structures and the flow field.

5. Methods of combining closed cycle MHD with fusion reactors.

In regard to the first item, after we observed recovery of β_{eff} up to 4 - 5, and also the enhancement of power output with a disk generator in the regime of fully ionized seed, we have conducted power generation experiments with an Ar/K linear Faraday generator under a seed fraction of 10^{-5}. Preliminary results obtained early in 1977 showed that σ_{app} increased up to 25 v/m when the seed was fully ionized.

With this encouraging result, we are now going to proceed to the second item. Calculation shows that when a loading factor

is high (0.7 - 0.8), the power density in a stabilized plasma with a small seed fraction is larger than that in a turbulent plasma with a large seed fraction. In order to demonstrate it experimentally, a series of power extraction experiments with a linear Faraday generator are being conducted for various seed fractions and loading factors using a shock heated Ar/K gas. In order to investigate the third item, we have already prepared the third shock tube, which is connected with a new disk generator. Experiments will be started in July 1977.

Experiments for the fourth item are in progress with an arc-heated wind tunnel and part of the results will be reported shortly. And, finally, concerning the last item, we have started experiments for a gas-blanketed plasma, which is contained in a small torus.

FACILITIES AND SYSTEM STUDIES

Summary of Proposed
Dutch MHD-Development Program

by
Robert A. van der Laken
Netherlands Energy Research Foundation, ECN
Petten, Holland

Introduction

Various studies of the future energy consumption in the Netherlands indicate a diminishing availability of natural gas for electricity production. Nuclear reactors alone will not be a sufficient substitute, (Figure 1). Coal, to be imported from other countries, will, therefore, become an important primary energy source in the next decades. Already now, the coal prices in Rotterdam are at least twice as high as in the United States. Combined with the expected real-price increase in the near future, there is certainly a need for high-efficiency power plants such as the MHD steam system.

There is another, maybe even more important, reason to develop advanced energy-conversion systems in the Netherlands. Today, the Netherlands is an energy-exporting country. This situation will very soon change, and so we are faced with the question of how to balance the energy import. New export markets for our industry are therefore needed. High-technology products like MHD components can open such markets. It is, therefore, proposed that the Dutch MHD development program emphasize the industrial aspect.

Goals

In view of the foregoing, it is clear that the main goal of the proposed Dutch MHD development program is:

- To provide the interested Dutch industry with the means to acquire know how and experience in the field of MHD - energy conversion.

More specifically, we should make possible the acquisition of know-how with respect to design and manufacture of large MHD components which, in the future for other advanced energy systems, could be of vital importance. In this way, bringing Dutch industry in a favorable position for international cooperation.

Scope

The present proposal is directed toward the technical demonstration of closed cycle MHD. The program should provide a data base for the decision to demonstrate the viability of the concept in a small power plant. Three main lines can be distinguished in the program:

1) Construction and operation of a Physical Demonstration Facility at the Technical University Eindhoven (already started).

2) Development and construction of superconducting magnets.

3.) Construction and operation of a Technical Demonstration Facility.

Not all components will be developed in Holland. Emphasis will be on superconducting magnets, on high-temperature heat exchangers, and on the material development for the channels.

The development of the Technical Demonstration Facility will consist of five phases (See Figure 2). After preliminary design studies, the design and construction of the Heat Production System consisting of the argon-heat exchanger, high-temperature valving and vacuum system, will be designed and constructed. Fuel will most probably be natural gas with additions to simulate coal firing. In separate installation, i.e., at the International Flame Research Foundation, Ymuiden, the influence of direct coal burning on the heat exchanger materials can be investigated. In a following phase, this Heat Production System will be extended with the argon and seed system, to complete the installation in what essentially can be called a zero-power MHD

plant. In this configuration, MHD-channels can be tested. In the final phase, a superconducting magnet will be installed to enable power operation.

Program Organization

The management of the program will be entrusted to the Netherlands Energy Research Foundation, ECN.

The Technical University Eindhoven is responsible for the construction and operation of the Physical Demonstration Facility.

Two Dutch industries, VMF-Stork and Holec, will be responsible for the superconducting magnet development, in cooperation with ECN, where part of the research will be carried out. In addition, VMF-Stork will be responsible for the heat exchanger development.

ECN will operate the TDF facilities, which will most likely be erected at its research center near the village Petten.

The total cost of the program is presently estimated at 70 million Dutch florins (30 million dollars) of which about 60% has to be financed by the Dutch government directly.
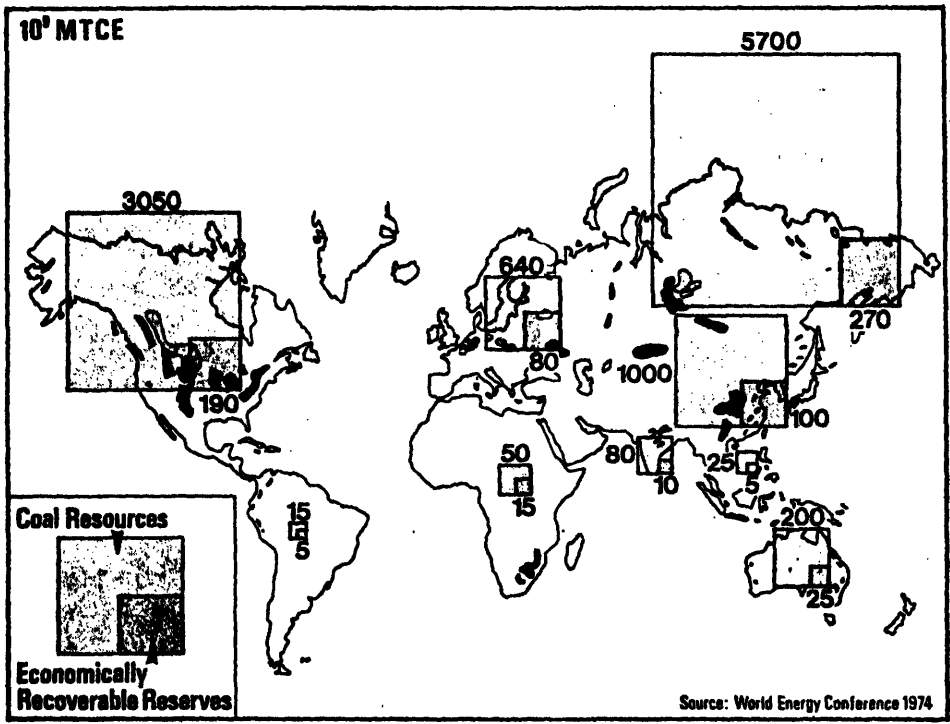
Figure 2. Coal resources and economically recoverable reserves.
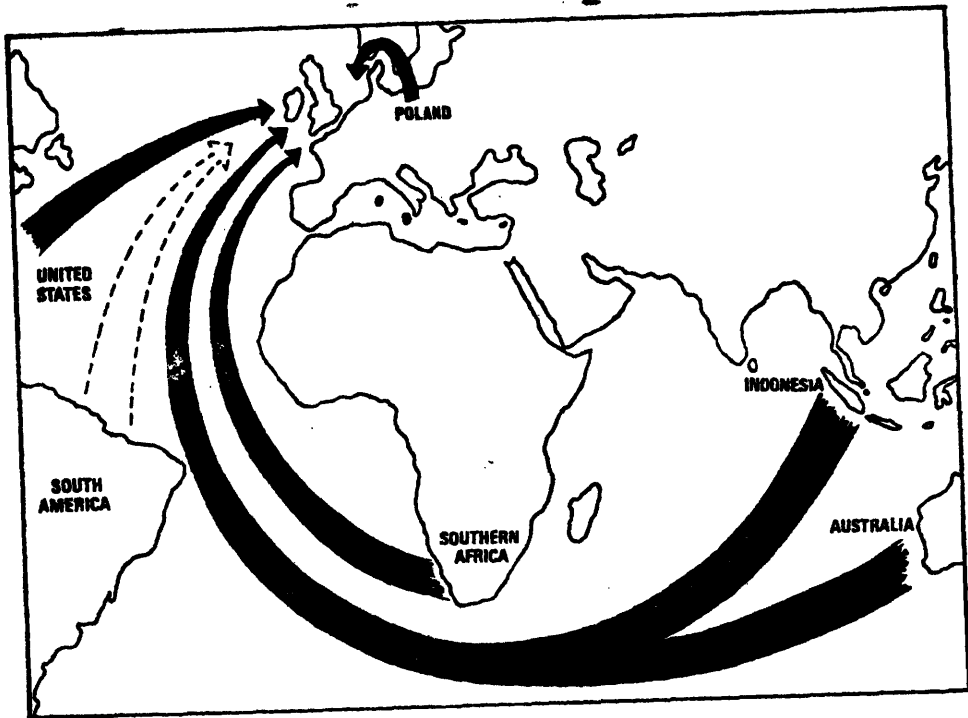
Figure 3. Possible coal flows to Western Europe.

DUTCH MHD-PROGRAMME
TDF-DEVELOPMENT PHASES

1977	1978	1979	1980	1981	1982	1983	1984	1985	1986

Fase 1
- System studies
- Mat. dev.

Fase 2
- Prel. design TDF
- Constr WPS
- Dev. PDF-magnet

Fase 3
- Design argon &
  seed-systems
- Operation WPS
- Constr. PDF-magnet
- Design TDF-magnet

Fase 4
- Operation TDF-o
  + MHD-channels
- Operation PDF-
  magnet
- Constr TDF-
  magnet

Fase 5
- Install. TDF-magnet
- Operation TDF-S

TIME SCHEDULE DUTCH MHD-PROGRAMME

15.5.77

MILESTONES	1976	1977	1978	1979	1980	1981	1982	1983	1984	1985	1986
	bouw PDE	system studies		design & constr. WPS		operation WPS	operation TDF-0		start TDF – operation		
Proposal Dutch progr.											
Discussion proposal											
Prel. studies											
Shocktube exp.											
Constr. PDF											
Dev. 2-dim. code											
Diffuser-code											
System studies											
Prel. design PDF-mag.											
PDF-experiments											
Des. & Constr WPS											
Operation WPS											
Constr argon/seed syst.											
Dev. PDF-magnet											
Constr. & Testing ditto											
Design TDF-magnet											
Constr. "											
Operation TDF-o											
Operation TDF-5											

−73−

EXHAUST ARGON GAS

DIFFUSER

MHD CHANNEL

CRYOGENIC MAGNET

CESIUM SYSTEM

COMBUSTION SYSTEM

HEAT EXCHANGER

EXHAUST COMBUSTION GAS

BYPASS

VACUUM SYSTEM

ARGON SYSTEM

5MW BLOW DOWN FACILITY
TH EINDHOVEN

STATUS OF THE MHD BLOW-DOWN EXPERIMENT
by
J. H. Blom
Eindhoven University of Technology
Eindhoven, Netherlands

The objectives of this project are stated as:

- the demonstration of an enthalpy extraction of 20% during 10 s,

- a study of the physical processes will occur in a closed cycle MHD generator with an input of 5 MWth and an operation time of 10 s,

- the verification and evaluation of the model which describes the behavior of the generator.

The design of the facility was started in March 1975. The funding from the Department of Economic Affairs was granted in September 1976.

The status of some major components will be mentioned in the next paragraphs (compare the figure).

Heat-exchanger

The design of a cored brick regenerative heater by Fluidyne Corporation has been completed. A theoretical model, which describes the axial temperature distribution during reheat and blow-down, has also been completed.

Argon supply

Long-term argon storage is in liquid form. The gaseous argon for a run is supplied from a sphere of 4 m^3 at a pressure of 100 bar.

Cesium injection

The injection of cesium employing an ultrasonically-generated aerosol is under investigation. Auxiliary experiments using water and freon show that droplet sizes in the range from 10 to 80 μm can be produced. A model which describes the evaporation of the cesium droplets in the hot argon flow, shows that these sizes are sufficiently small to ensure that cesium will enter the generator in the vapor phase. The influence of the velocity and pressure of the argon flow has been investigated. The size of the cesium injection module is currently under investigation. The cesium storage system has been designed and is now in the construction phase.

Generator channel

The first generator channel to be tested diverges from 0.15×0.05 m^2 to 0.15×0.18 m^2 over a length of 0.8 m. The operation with stagnation pressures from 7 to 10 bar and stagnation temperatures between 2000 K and 1800 K will be investigated. The geometrical design of the channel is checked with respect to the sensivity for small changes in parameters as voltage drops, magnetic induction, stagnation temperature, etc. The experiments at low temperatures performed in the shock tunnel MHD generator and reported at the Philadelphia Meeting showed that the model did not account for the inlet relaxation process and boundary layer separation. Further experiments have shown that the inlet relaxation length decreases by applying appropriate preionization. The generator will have rod type electrodes to prevent boundary layer separation. Auxiliary experiments are performed to test candidate materials for the construction of the channel. The thermal shock resistance of materials is tested in a combustion gas flow, which simulates the 1 min argon blow-down conditions. The integrity of the material with respect to cesium at various temperatures is tested in a separate experiment.

Magnet

The facility will use an cryogenically cooled magnet with a maximum induction of 5 T in a warm bore with a size of 0.35 x 0.35 x 1 m^3. This magnet is under design at I.R.D. in Newcastle upon Tyne; the design will be completed next July.

The first runs are scheduled in the fall of 1978.

SOME PROBLEMS CAUSED BY THE USE
OF THE IONIZABLE SEED IN MHD GENERATORS
OF CLOSED CYCLE

by

I. L. Mostinsky

I.V.A.N.

Moscow, U.S.S.R.

A system of input-output of ionizable seed in energy MHD generators of closed cycle is considered in general. The difficulties of insuring the homogenuous distribution of seed in the entrance of the MHD generator, of getting the fullest condensation of cesium vapor in the condenser and of getting a good degree of catching the created fog are discussed.

The considerable complication of the considered problem is pointed out while using the organic fuel. Attention is drawn to the necessity of conducting pertinent investigations in the general cycle of investigations on MHD generators of closed cycle.

CLOSED CYCLE MHD PROGRAM AT NASA LEWIS RESEARCH CENTER

by

Ronald J. Sovie

NASA Lewis Research Center

Cleveland, Ohio

Although the closed-cycle MHD (CCMHD) program at Lewis does encompass systems studies of these systems and the layout of program plans for the development of CCMHD power plants, the main emphasis is presently on the experiments in the NASA closed-loop facility.

The goal of this experimental program is to demonstrate non-equilibrium MHD performance at power densities of 10-20 MW/M^3, initially for periods of minutes and ultimately for hundreds of hours in a realistic environment. The experiments are performed in a closed-loop, steady-state facility with hot generator walls to better simulate the conditions under which a real generator must perform. This program complements the shock-tube programs aimed at demonstrating large enthalpy extraction ratios and reasonable turbine efficiencies and can supply much basic system and design information useful for both future longer duration blowdown experiments and possible future steady-state power systems.

In the program at Lewis we have overcome many of the problems associated with the successful operation of a steady-state facility at temperatures of 2000-2100K. We have run many loop components for thousands of hours and have run MHD channels for hundreds of hours of thermal operation and hundreds of cesium injection tests without any problems.

Experiments have been performed using various working fluids at a variety of operating conditions. The MHD generator performance has steadily increased in the past few years although we

have not as yet obtained any non-equilibrium MHD performance. Consequently, we have been decreasing the MHD channel dimensions to allow operation at higher Mach numbers and increase the probability of obtaining non-equilibrium performance.

At present we are running a 3.8x11.4 cm MHD channel at T_s = 2060K and M = 0.36 using a helium-cesium working fluid. The best results obtained in this channel, to date, are for tests using 14 electrodes. In these tests V_F = 200 V (1750 V/M), V_H = 460 V (1450 V/M), P/V = 1.7 MW/M^3, and the total power output was 2.4 KW.

Data analysis indicates that the present performance is limited by low values of the Hall leakage resistance and resistive losses at the electrode boundary layers. The facility is presently being modified to greatly increase the Hall leakage resistance values and allow operation of the heater at 5 kV to ground. The MHD channel is being modified to run at Mach numbers up to 0.8. It is expected that non-equilibrium performance will be obtained once the changes are incorporated into the facility.

ROUND TABLE DISCUSSION

The Round Table Discussion covered all aspects of closed cycle MHD power generation. It was remarked that:

1. Non-equilibrium generators have clearly demonstrated their ability for enthalpy extraction in shock tunnel experiments, and there is an urgent need for similar demonstrations in large blow-down facilities. Favorable isentropic and electrical efficiency measurements were made in the MIT disk generator with swirl driven by hot argon. Similar measurements are needed to evaluate the performance of linear generators.

2. Long duration materials tests are needed to be performed in a facility with thermal power of a few MW.

3. The demonstration of the high-temperature heat exchangers remains a primary objective. For the U.S., the demonstration of heat exchangers fired by coal is particularly important.

4. The problems of seed injection and seed recovery need to be comprehensively studied. Engineering solutions to these problems have to be demonstrated.

5. System studies of MHD Closed Cycle MHD power plants have to be pursued. Such studies should emphasize economic plant size, plant configuration and plant availability.

6. It was unanimously agreed that this type of workshop provides a unique opportunity to discuss problems in depth and to provide a platform for a free exchange of information and for positive critique of new concepts.

Distribution

1977 CLOSED CYCLE MHD SPECIALIST MEETING
PROPOSED LIST OF INVITEES

International Atomic Energy Agency

Dr. V. Chernyshev
Division of Nuclear Power Reactors
International Atomic Energy Agency
Karntner Ring 11
P.O. Box 590
A-1011
Vienna, Austria

European Nuclear Energy Agency

Dr. W. Hausserman
European Nuclear Energy Agency
O.E.C.D.
38, Blvd. Suchet
F-75 PARIS 16e
France

Argentina

Dr. Naum Fraidenraich
Observatoria Nacional de Fisica
   Cosmica de San Miguel
Avda. Mitre 3100
San Miguel (F.C.G.S.M.)
Argentina

Australia

Prof. H. K. Messerle
University of Sydney
Head, School of Elecrical Engineering
NWS 2074
Sidney, Australia

France

Mr. R. Bidard
Cie Electro-Mecanique
12 Rue Portalis
75008 Paris
France

France (cont'd.)

Prof. E. Brocher
Institut de Mecanique des Fluides
1 Rue Honnorat
F-13 Marseille   13003
France

Dr. J. P. Caressa
Institut de Mecanique des Fluides
1 Rue Honnorat
Marseilles 13003
France

Mr. P. Ricateau
Chef de Groupe de Conversion M.H.D.
Centre d'Etudes Nucleaires de Saclay
F-91 GIF-SUR-YVTETTE
France

Mr. M. Sterlini
Cie Electro-Mecanique
12 Rue Portalis
75008 Paris
France

Prof. J. Valensi
Directeur de l'Institut de Mecanique
   des Fluides
1 Rue Honnorat
F-13 Marseille 13003
France

Italy

Dr. M. E. Bertolini
Comitato Nazionale per l'Energia
Nucleare - Laboratorio Conversione
Diretta
P.O.B. 65
Frascati (Roma)
Italy

Italy (Cont'd.)

Dr. Ing. F. Negrini
Instituto di Elettrotechnica
Facolta di Ingegneria
Via Risorgimento 2
I-40136 Bologna
Italy

Ing. Enrico Sobrero
Assistente di Impianti Nucleari
Facolta di Ingegneria
Via Risorgimento 2
I-40136 Bologna
Italy

Prof. Dr. R. Toschi
Director of Direct Conversion Lab
Comitato Nazionale per l'Energia
    Nucleare
P.O.B. 65
Frascati (Roma)
Italy

Dr. V. Zampaglione
Laboratory of Direct Conversion
C.N.E.N.
P.O.B. 65
Frascati (Roma)
Italy

Japan

N. Kayukawa
Department of Nuclear Engineering
    and Science
Hokkaido University
Sapporo
Japan

M. Miyata
Department of Mechanical Engineering
Kelo University
832 Kiyoshi-Cho, Kohoku-Ku
Yokohama
Japan

Prof. S. Shioda
Tokyo Institute of Technology
OhOkayama, Meguro-Ku
Tokyo
Japan

Japan (Cont'd.)

K. Yoshikawa
Research Associate
Corpuscular Engineering Laboratory
Institute of Atomic Energy
Kyoto University
Uji, Kyoto 611
Japan

The Netherlands

J. Blom
Eindhoven University of Technology
Postbus 513
Eindhoven
Netherlands

Dr. J. W. Houben
Group of Energy Conversion
Department of Electrical Engineering
Technishce Hogeschool Eindhoven
Insulindelaan 2
Eindhoven
Netherlands

W. F. H. Merck
Eindhoven University of Technology
P. O. Box 513
Eindhoven
Netherlands

Prof. L. H. Th. Rietjens
Department of Electrical Engineering
Eindhoven University of Technology
Postbus 513
Eindhoven
Netherlands

Poland

Dr. W. S. Brzozowski
Plasma Physics and Technology Lab.
Institute for Nuclear Research
Swierk k/Otwocka
Warsaw
Poland

Dr. L. Celinski
Plasma Physics and Technology Lab.
Institute for Nuclear Research
Swierk k/Otwocka
Warsaw
Poland

Distribution (continued)

United States of America (Cont'd.)

Dr. William D. Jackson, Director
Division of MHD
Fossil Energy
Department of Energy
20 Massachusetts Ave., N.W.
Washington, D.C.   20545

Dr. R. Johnson
Montana State University
Butte, Montana   59701

Prof. J. L. Kerrebrock
Gas Turbine Lab, 31-264
Department of Aeronautics and
   Astronautics
Massachusetts Institute of Technology
Cambridge, Massachusetts   02139

Dr. James Klepeis
AVCO Everett Research Labs
Revere Beach Parkway
Everett, Massachusetts

Prof. J. F. Louis
Gas Turbine Lab, 31-254
Department of Aeronautics and
   Astronautics
Massachusetts Institute of Technology
Cambridge, Massachusetts   02139

Dr. Charles H. Marston
General Electric Company
Space Sciences Laboratory
VFSC - Rm. L9515
P.O. Box 8555
Philadelphia, Pennsylvania   19101

Prof. M. Mitchner
Mechanical Engineering Department
Thermal Sciences Division
Stanford University
Stanford, California   94305

Prof. S. I. Pai
Fluid Mechanics Institute
University of Maryland
College Park, Maryland   20742

Dr. C. H. T. Pan
Shaker Research Corporation
Northway 10
Executive Park
Ballston Lake, N.Y.   12019

Dr. Richard Y. Pei
Rand Corporation
2100 M Street, N.W.
Washington, D.C.   20037

Dr. Michael Petrick
Argonne National Laboratory
9700 South Cass Avenue
Building 335
Argonne, Illinois   60439

Mr. John A. Satkowski
Director, Power Program
Office of Naval Research - Code 473
Department of the Navy
800 N. Quincy Street
Arlington, Virginia   22217

G. R. Seikel
NASA Lewis Research Center
21000 Brookpark Road
Cleveland, Ohio   44135

Dr. R. V. Shanklin
Division of MHD
Fossil Energy
Department of Energy
20 Massachusetts Avenue, N.W.
Washington, D.C.   20545

Dr. M. Sluyter
Division of MHD
Fossil Energy
Department of Energy
20 Massachusetts Avenue, N.W.
Washington, D.C.   20545

Mr. J. M. Smith
NASA Lewis Research Center
21000 Brookpark Road
Cleveland, Ohio   44135

Dr. R. J. Sovie
NASA Lewis Research Center
21000 Brookpark Road
Cleveland, Ohio   44135

Distribution (continued)

Sweden

Prof. Dr. J. Braun
Director of the Institute for General
    Physics
A.B. Atomenergi
Studsvik
Fack
S-611 01 Nykoping
Sweden

H. Zinko
A.B. Atomenergi
Studsvik
Fack
S-611 01 Nykoping 1
Sweden

Switzerland

Dr. P. Jeanmaire
WIFO - Wissenschaflichen Forschungs
Institut AG
Binzstrasse 18
CH-8045 Zurich
Switzerland

Dr. V. Stingelin
Scientific Associate to the Head of
    Engineering Department
Battelle-Geneva Research Center
7, Rte. de Drize
CH-1227 Carouge-Geneva
Switzerland

United Kingdom

Dr. I. R. McNab
International Research and Devel-
    opment Co., Ltd.
Fossway, Newcastle Upon Tyne
England NE62YD

United States of America

Mr. J. A. Burkhart
NASA Lewis Research Center
21000 Brookpark Road
Cleveland, Ohio 44135

United States of America (Cont'd.)

Dr. Charles S. Cook
General Electric Company
Space Sciences Laboratory
VFSC - Rm. L9517
P.O. Box 8555
Philadelphia
Pennsylvania 19101

Mr. Donald L. DeDominicis
General Electric Company
Space Sciences Laboratory
FVSC - Rm. L9521
P.O. Box 8555
Philadelphia
Pennsylvania 19101

Dr. Sterge Demetriades
STD Research Corporation
P.O. Box C
Arcadia, California 91006

Prof. R. H. Eustis
Thermosciences Division
Mechanical Engineering Department
Stanford University
Stanford, California 94305

Dr. O. G. Farah
The MITRE Corporation
1820 Dolley Madison Boulevard
McLean, Virginia 22101

Dr. Lawson P. Harris
General Electric Co.
Corp. Research and Development
P.O. Box 8 - Bldg. K-1
Schenectady, New York 12301

Mr. R. D. Hay
Magnetic Engineering Associates
169 Bent Street
Cambridge, Massachusetts 02141

Prof. William F. Hughes
Department of Mechanical Engineering
Carnegie-Mellon University
Schenley Park,
Pittsburgh, Pennsylvania

United States of America (Cont'd.)

Prof. M. E. Talaat
Professor of Mechanical Engineering
University of Maryland
College Park, Maryland   20742

Mr. Eric Tate
General Electric Company
Space Sciences Laboratory
VFSC - Rm. L9515
P.O. Box 8555
Philadelphia, Pennsylvania   19101

Dr. Fred Tsu
Westinghouse Electric Corporation
Beulah Road, Churchill Borough
Pittsburgh, Pennsylvania   15235

Dr. Jack Vanderryn
Director, International Affairs
Department of Energy
20 Massachusetts Avenue
Washington, D.C.   20545

Mr. W. H. Wilkinson
Battelle Columbus Laboratories
505 King Avenue
Columbus, Ohio   43201

Mr. J. R. Williams
Georgia Institute of Technology
Atlanta, Georgia

Dr. Bert Zauderer
Manager, MHD Programs
General Electric Company
Space Sciences Laboratory
VFSC - Rm. L9513
P.O. Box 8555
Philadelphia, Pennsylvania   19101

Mr. Paul Zygelbaum
Electric Power Research Institute
3412 Hillview Avenue
Cleveland, Ohio   44135

U.S.S.R.

D. A. Bout
Moscow Aviation Institute
Moscow
U.S.S.R.

Dr. S. A. Medin
Institute of High Temperatures
Korowinskoye Road
127412 Moscow I-412
U.S.S.R.

Dr. A. V. Nedospasov
Institute of High Temperature
Academy of Science
Moscow
U.S.S.R.

Dr. A. V. Ouchasrenko
Institute of High Temperatures
Moscow E-250 Krasnokazarmennasa
179
U.S.S.R.

Prof. A. E. Scheindlin
Institute of High Temperatures
Korowinskoye Road
127412 Moscow I-412
U.S.S.R.

Prof. E. P. Velikov
Deputy Director of the Atomic
    Energy Institute
Moscow
U.S.S.R.

Distribution (continued)

MHD DISTRIBUTION LIST

Aerodyne Research Inc.
Bedford Research Park
Crosby Drive
Bedford, Massachusetts 017030

Mr. Robert F. Cooper
Technical Manager, Plasma Dynamics
Aerospace Power Division
Air Force Aero Propulsion Laboratory
Wright Patterson A.F.B., Ohio 45433

Mr. Elton R. Thompson
Research and Development Division
Directorate of Technology
Department of the Air Force
Headquarters Arnold Engineering Center
Arnold Air Force Station,
Tennessee 37389

Dr. W. C. Redman
Argonne National Laboratory
9700 South Cass Avenue
Argonne, Illinois 60439

Mr. Gregory B. Barthold
Aluminum Company of America
1200 Ring Bldg.
Washington, D.C. 20036

Dr. R. W. Detra
Avco-Everett Research Laboratory, Inc.
2385 Revere Beach Parkway
Everett, Massachusetts 02139

Mr. J. Lambert Bates
Battelle Pacific Northwest
    Laboratories
P.O. Box 999
Richland, Washington 99352

Mr. Paul Zyglebaum
Electric Power Research Institute
3412 Hillview Avenue
Palo Alto, California 94304

Dr. D. Bienstock
Energy Research & Development
    Administration
Pittsburgh Energy Research Center
3800 Forbes Avenue
Pittsburgh, Pennsylvania 15213

Mr. L. Frame
FluiDyne Engineering Corporation
5900 Olson Highway
Minneapolis, Minnesota 55422

Mr. C. S. Cook
General Electric Company
Space Sciences Laboratory
Space Division
P.O. Box 8555
Philadelphia, Pennsylvania 19101

Dr. Bert Zauderer
General Electric Company
Space Sciences Laboratory
Space Division
P.O. Box 8555
Philadelphia, Pennsylvania 19101

Mr. D. F. Crego
Gilbert Associates, Inc.
P.O. Box 1498
Reading, Pennsylvania 19603

Mr. Richard J. Thome
Magnetic Corporation of America
179 Bear Hill Road
Waltham, Massachusetts 02154

Prof. J. F. Louis
Room 31-254
Department of Aeronautics and
    Astronautics
Massachusetts Institute of Technology
Cambridge, Massachusetts 02139

Materials Consultants, Inc.
2150 South Josephine Street
Denver, Colorado 80210

Mr. T. R. Brogan, President
MEPPSCO
141 Pearl Street
Boston, Massachusetts 02110

Mr. David L. Murphee
Mississippi State University
Mississipp State, Mississippi 39762

Distribution (continued)

MHD DISTRIBUTION LIST (CONT'D.)

Mr. Wesley Ennis
Montana Energy and MHD Research and
    Development Institute
P.O. Box 3708
Butte, Montana 59701

Dr. J. Plunkett
Montana Energy and MHD Research and
    Development Institute
P.O. Box 3708
Butte, Montana 59701

Montana State University
Bozeman, Montana 59715

Montana Tech
Butte, Montana 59701

Mr. Frank Shafran
Ralph M. Parson Company
Pasadena, California 91124

Dr. S. T. Demetriades, President
STD Research Corporation
P.O. Box "C"
Arcadia, California 91006

Prof. R. Eustis
Leland Stanford Jr. University
Stanford, California 94305

Mr. Uwe Zitzow
Tennessee Valley Authority
503 Power Building
Chattanooga, Tennessee 37401

Mr. S. J. Schneider
U. S. Department of Commerce
National Bureau of Standards
Washington, D. C. 20234

Prof. J. B. Dicks, Director
Energy Conversion Division
University of Tennessee Space
    Institute
Tutlahoma, Tennessee 37388

Prof. Ivan B. Cutler
University of Utah
College of Engineering
Department of Material Science and
    Engineering
Salt Lake City, Utah 84112

Mr. W. E. Young, Manager
MHD Systems Research
Westinghouse Electric Corporation
Research and Development
Beulah Road
Pittsburgh, Pennsylvania 15235

Mr. Robert F. Cooper
AFAPL/POD
Department of the Air Force
Air Force Wright Aeronautical
    Laboratories (AFSC)
Air Force Aero Propulsion Laboratory
Wright Patterson Air Force Base, Ohio 45433

Mr. Craig Maxwell
STD Research Corporation
1143 New Hampshire Ave., N.W.
Washington, D.C. 20037

Reynolds Metals Co.
Reduction Research Division
MHD Research Department
P.O. Box 191
Sheffield, Alabama 35660

The Rand Corporation
1700 Main Street
Santa Monica, California 90406

Mr. K. J. Touryan
Sandia Laboratories
Alburquerque, New Mexico 87115

(All attendees will also receive
a copy)